Nucleotide excision repair at the single-molecule level : analysis of the E. coli UvrA protein

Wagner, K.

Role of the insertion domain and the zinc-finger motif of *Escherichia coli* UvrA in damage recognition and ATP hydrolysis

Chapter 5

Koen Wagner, Geri F. Moolenaar and Nora Goosen

Laboratory of Molecular Genetics, Leiden Institute of Chemistry, Leiden University, Einsteinweg 55, 2333 CC, Leiden, the Netherlands

ABSTRACT

UvrA is the initial DNA damage-sensing protein in bacterial nucleotide excision repair (NER). The active form of UvrA is a dimer capable of binding to a wide variety of lesions, after which it hands off the damaged site to UvrB. The UvrA monomer consists of two ATPase domains, both belonging to the family of ATP-binding cassette domains. Three structural domains are inserted in these ATPase domains: the insertion domain (ID) and UvrB binding domain (both in ATP binding domain I) and the zinc-finger motif (in ATP binding domain II). In this paper we analyze the function of the ID and the zinc finger motif in damage specific binding of *Escherichia coli* UvrA.

We show that the ID is not essential for damage discrimination, but stabilizes UvrA on the DNA, most likely because the two IDs form a clamp around the DNA helix. Upon detection of a damage the ATPase of UvrA is activated which stabilizes the interaction of the protein with DNA containing a non-bulky lesion. Two conserved arginine residues of the ID appear essential for this stabilization. We present evidence that these residues contact the phosphate backbone of the DNA, leading to strand separation after the ATPase-driven movement of the IDs.

The zinc-finger motif is shown to be an important domain for the transfer of the damage recognition signal to the ATPase of UvrA. In the absence of this domain the coupling between DNA binding and ATP hydrolysis is completely lost. Substitution of the phenylalanine residue in the tip of the zinc-finger domain with alanine resulted in a protein in which the ATPase was already triggered when binding to an undamaged site. As the zinc-finger motif is connected to the DNA binding regions on the surface of UvrA, this strongly suggests that damage-specific binding to these regions results in a rearrangement of the zinc-finger motif, which in its turn activates the ATPase. We present a model how damage recognition is transmitted to activate ATP hydrolysis in ATP binding domain I of the protein.
Remarkably, deletion of the ID generates a phenotype in which UV-survival strongly depends on the presence of photolyase. We present evidence that photolyase stimulates UvrA to bind CPD-lesions by forming a ternary complex where both proteins are bound at the site of the lesion.

INTRODUCTION

Nucleotide excision repair (NER) is a universal DNA repair pathway that has the unique property of being able to remove a large variety of structurally unrelated lesions from the genome. In bacterial NER, recognition of DNA damage and subsequent incision is performed by three proteins: UvrA, UvrB and UvrC [1,2].

In the current model for bacterial NER, UvrA functions in the first steps of the repair reaction: Two UvrA molecules form the UvrA dimer complex, which is the active form of UvrA [3,4]. The UvrA dimer binds two UvrB proteins to form the $UvrA_2B_2$-complex [5]. In this complex, the two UvrA subunits probe DNA for damage. The UvrA dimer likely recognizes unwound DNA, as UvrA has higher affinity for DNA structures that resemble single-stranded DNA, such as single-strand/double-strand DNA junctions or DNA ends [3,4,6]. Upon detecting a potential lesion, UvrA tries to load UvrB to the damaged DNA. After UvrB is successfully positioned at the damaged site the UvrA subunits dissociate, thus leaving a complex of two UvrB subunits: the pre-incision complex. This complex is the target for UvrC binding, which displaces one UvrB subunit and then incises the damaged DNA strand first 3' to the lesion and then on the 5' side [1,2].

The *Escherichia coli* UvrA protein, which has a size of 104 kDa, contains two ATPase domains that both belong to the ABC (ATP Binding Cassette) class of ATPases [7] and are essential for repair [8-10]. The activities of the two ATPase domains are tightly coupled, indicating that the two domains function as one cooperative module [10].

In the absence of DNA, ATP hydrolysis stabilizes the UvrA dimer [10]. In its active form, the UvrA dimer likely contains a mixture of ATP and ADP divided over its four ATPase domains, as in the presence of either a non-hydrolyzable ATP analog or ADP its specificity for DNA damage is reduced [4,11]. Upon binding damaged DNA, the ATPase activity of *E. coli* UvrA is stimulated and this is proposed to facilitate opening of the DNA strands around a lesion, thereby stabilizing the UvrA-complex on non-bulky lesions and facilitating DNA binding of UvrB [10].

In addition to the two ATPase domains, three functional domains, each coordinated by a zinc-binding module, were identified in the crystal structure of *Bacillus stearothermophilus* UvrA (Figure 1A): The UvrB-binding domain, the insertion domain (ID) and the zinc-finger motif [12]. Similar to the structures of other ABC ATPases [13], these functional domains are inserted within the ATPase domains of UvrA; suggesting that the role of each functional domain is controlled by ATP binding and hydrolysis. ATPase domain I contains the UvrB-binding domain and the ID, while the zinc-finger motif is inserted in ATPase domain II [12]. Recently also the structure of a UvrA homolog, lacking the UvrB-binding domain (UvrA2), from *Deinococcus radiodurans* was determined [14]. In this structure (Figure 1D), the two monomers have their insertion domains positioned in a more closed configuration than in *B. stearothermophilus* UvrA (Figure 1C). In both structures however, the IDs have an almost perpendicular orientation towards the DNA binding patches located on the ventral surface of the UvrA dimer. These patches consist of several positively charged surface-exposed residues that were shown to contribute to DNA binding [12,15].

The zinc-finger motif of UvrA is a small domain which structure does not directly resemble the generic zinc-finger structure [12]. Also, in contrast to other zinc-finger domains, the zinc-finger motif of UvrA does not bind DNA by itself [16]. Instead, this motif was proposed to indirectly regulate damage-specific binding [16]. In the structure of *B. stearothermophilus* UvrA, the two phenylalanine residues, positioned at the extreme tip of the zinc-finger motifs, are in close proximity to each other, suggesting that the two residues can interact (Figure 1B).

In *E. coli* UvrA, the ID consists of approximately 100 amino acids. This domain is however poorly conserved between different bacterial species, both in size and in amino acid composition [17]. The function of the ID is unclear as different studies have yielded contradictory results. Pakotiprapha *et al.* [12] have shown that *in vitro* the ID of *B. stearothermophilus* UvrA is not required for UvrABC-mediated incision of DNA containing a site-specific lesion.

For the *D. radiodurans* UvrA2 protein, however, the ID was proposed to be essential for damage discrimination since a mutant lacking the domain lost the ability to discriminate between damaged and non-damaged DNA [14].

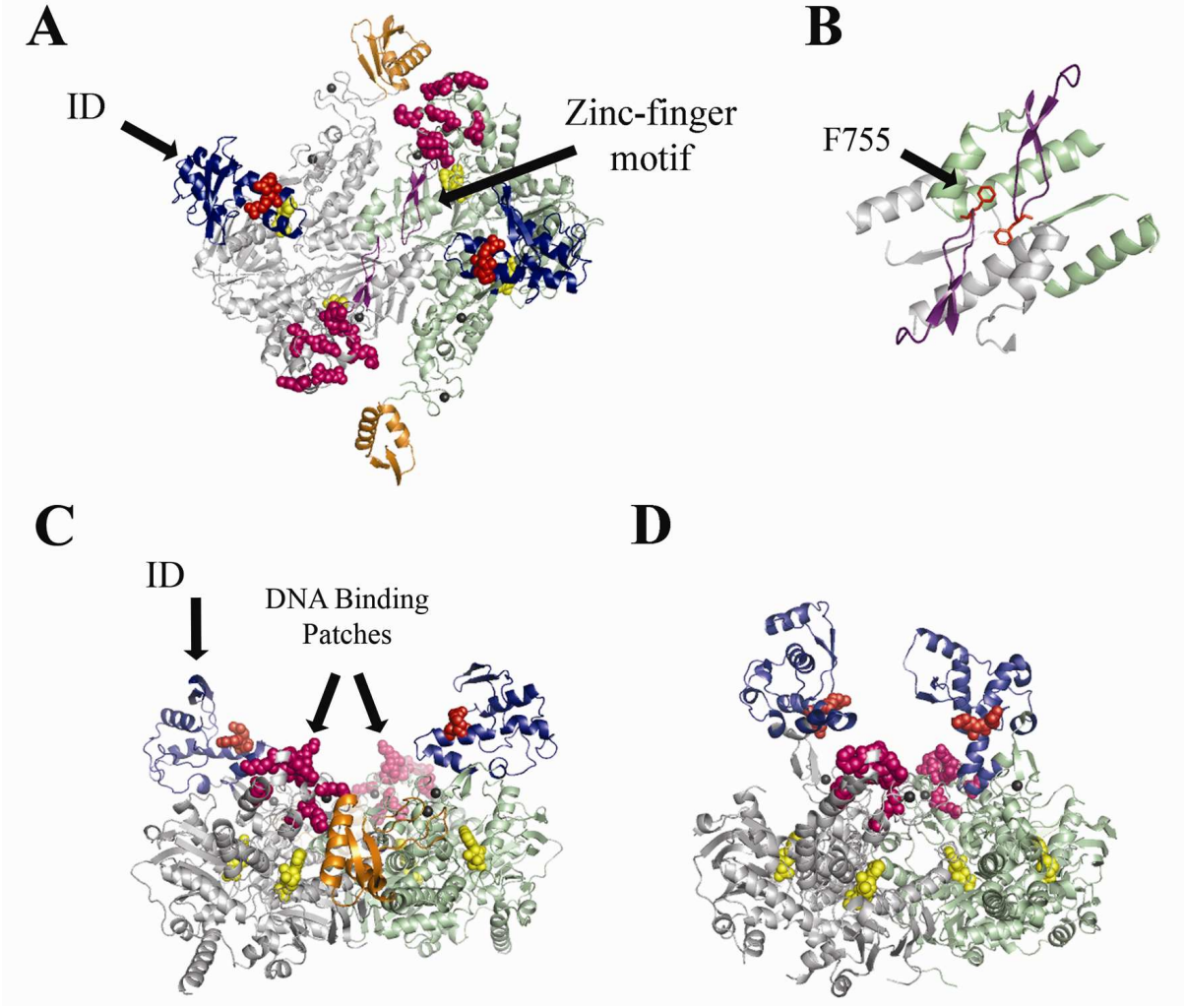

Figure 1: Structure of UvrA

(**A**) Top-view on the crystal structure of *B. stearothermophilus* UvrA (PDB entry 2R6F), showing the positions of the ID and the zinc-finger motif.

(**B**) Zoom in on the zinc-finger motif and the dimer interface of UvrA. In this panel, residue F751 (F755 in *E. coli* UvrA) is shown in red.

Panels (**C**) and (**D**) show front views of the crystal structures of the ADP-bound dimer form of *B. stearothermophilus* UvrA (**C**) and of *D. radiodurans* UvrA2 (**D**) (PDB entries 2R6F and 2VF7, respectively), indicating the orientation of the ID towards the DNA binding patches of UvrA.

In all structures monomer 1 is shown in gray and monomer 2 is colored light green. In both monomers, the insertion domain is shown in blue; the two conserved arginine residues within the insertion domain (R381 and R382 in *B. stearothermophilus* UvrA) are shown as red spheres. In (**A**) and (**B**), the zinc-finger motif of UvrA is colored violet. The DNA binding patches of UvrA are shown as pink spheres. The UvrB-binding domain of *B. stearothermophilus* UvrA is colored orange. Bound Zn^{2+} is shown as gray spheres; bound ADP is shown as yellow spheres. These images were made using PyMOL software (DeLano Scientific).

We have further analyzed the functions of the ID and the zinc-finger motif in the *E. coli* UvrA protein. Here, we show that the zinc-finger motif is part of the dimer interface of UvrA, contributing to the proper orientation of the two UvrA monomers in the dimer complex. We also show that the zinc-finger motif is an important mediator for transfer of the damage recognition signal to ATP hydrolysis.

Analysis of UvrA ID mutants revealed that this domain is not essential for damage recognition, but it does stabilize the UvrA complex on damaged DNA and helps the ATPase-mediated strand separation on non-bulky lesions. Based on our results, we propose a new model for DNA binding and damage recognition by UvrA.

MATERIALS AND METHODS

Proteins

Four UvrA mutants were constructed and purified: UvrA ΔID, in which amino acids 288 to 402 of UvrA were replaced by a two amino acid (GT) flexible linker, UvrA RR (in this mutant amino acids R383 and R384 were both substituted with alanine), UvrA F755A and UvrA ZnG, in which amino acids 750 to 760 were replaced by a single glycine residue. All mutations were introduced into the pTTQ-A9 expression plasmid [18] by PCR. (Mutant) UvrA, UvrB and UvrC proteins were purified as described [19]. UVDE was purified as described [20]. Purified *E. coli* CPD-photolyase was a kind gift from Andre Eker. T4 endonuclease V was a gift from Tineke de Ruijter.

UV-survival assay

For *in vivo* studies, the *uvrA* mutations were inserted into the pSC101-derived pNP120 plasmid [21], which carries the *uvrA* gene under control of its native promoter. The pNP120-derived plasmids expressing (mutated) UvrA were introduced into CS5865 (GM1 Δ*uvrA*, our lab) or CS5900 (GM1 Δ*uvrA*Δ*phr*, our lab). Transformants were grown to an OD_{600} of 0.3. This culture was diluted 10 times, after which 1 μl drops were deposited onto LB-agar plates, which were irradiated with the indicated doses of UV-light. The plates were incubated overnight in the dark, at 30 °C.

DNA substrates

The 678 bp DNA fragments without damage or containing a Cholesterol or CPD lesion were prepared as described [10]. For radioactive labeling of the 678 bp substrates at the 5' side, the DNA was heated to 80 ºC in 50 mM Tris (pH 9.5) containing 10 mM $MgCl_2$ and 2 pmol γ^{32}P-ATP (7000 Ci/mmol), followed by quickchill on ice. Next 5 mM DTT and 10 units of polynucleotide kinase were added and the sample was incubated at 37 ºC for 45 minutes. The reaction was terminated by adding 25 mM EDTA and heating at 80 ºC for 10 minutes. The DNA was purified using a G50 spin column. DNA concentrations were adjusted to 4 fmol/µl. The presence of the Cholesterol lesion at position 340, which is located in an *EcoRV* recognition sequence, was verified by digestion with EcoRV. The presence of the CPD lesion at positions 335 and 336, which are not part of a sequence that can be targeted by a restriction enzyme, was verified by incision with UVDE (as described in [20]) and T4 endonuclease V. Incision with T4 endonuclease V was performed in T4-endo buffer (50 mM KPO_4 pH 6.5, 10 mM EDTA, 50 mM NaCl + 1 mM β-Mercaptoethanol).

Incision assay

Radioactively labeled DNA (0.4 nM) was incubated with 2.5 or 7.5 nM UvrA, 400 nM UvrB and 25 nM UvrC in 20 µl UV-endo buffer. The incubation time varied with the used substrate, Cholesterol-DNA was incubated for 15 min at 37 °C and CPD-DNA was incubated for 30 min. After incision, the DNA was precipitated with ethanol and analyzed on 3.5 % denaturing polyacrylamide gels as described. When indicated, 50 nM photolyase was added before the addition of UvrABC. Samples containing photolyase were pre-incubated in the dark (10 min, 22 °C). Samples containing photolyase were kept in the dark until the reactions were terminated. The amounts of incised and unincised DNA were quantified as described [22].

ATPase assay

Samples were incubated for 20 minutes at 37 ºC in ATPase-endo buffer (50 mM Tris-HCl, pH 7.5, 15 mM $MgCl_2$, 100 mM KCl, 0.1 mg/ml BSA, 10 % glycerol and 0.5 mM ATP plus 0.1 µCi γ^{32}P-ATP (3000 Ci/mmol)). Reaction mixtures contained 30 nM UvrA. When indicated, supercoiled pUC18 DNA was added in a final concentration of 4 ng/µl. For the preparation of UV-damaged DNA, pUC18 was irradiated with UV-light. When indicated, 50 nM photolyase was added before the addition of UvrA. Samples containing photolyase were pre-incubated in the dark (10 min, 22 °C).

Samples containing photolyase were kept in the dark until the reactions were terminated. ATPase activity of (mutant) UvrA was measured by counting the production of ^{32}P-phosphate from γ^{32}P-ATP, as described [23].

Gel retardation assay

Gel retardation assays were performed as described [19]. UvrA was incubated in UV-endo buffer (with or without 1 mM ATP) for 5 min at 37 °C, after which DNA was added to the samples. Samples containing both UvrA and UvrB were incubated in UV-endo buffer + 1 mM ATP (5 min, 37 °C) before addition of DNA. After 10 min of incubation with DNA, samples were separated on 3.5 % native polyacrylamide gels containing 10 mM $MgCl_2$ and, when indicated, 1 mM ATP.

Western Blots

For the Western Blots, 100 nM of UvrB was incubated with the indicated amounts of UvrA in UV-endo buffer. Reaction mixtures were separated on 3.5 % native polyacrylamide gels containing 10 mM $MgCl_2$ and 1 mM ATP. After blotting of the proteins on a nitrocellulose membrane, the membrane was incubated with rabbit UvrB antibody (described in [19]) and the secondary antibody goat anti-rabbit alkaline-phosphatase (GARAP) in blocking buffer (1 mg/ml BSA). The presence of UvrB-coupled GARAP was detected by staining with nitro-blue tetrazolium (NBT) plus 5-bromo-4-chloro-3-indolyl phosphate (BCIP) as described [10].

Atomic Force Microscopy Imaging

AFM imaging of UvrA and UvrA-DNA complexes was performed as described [4]. Imaging was performed with a Nanoscope III instrument (Digital Instruments), equipped with an E-scanner, using tapping mode in air. OMCL-AC240TS MicroCantilever tapping mode cantilevers (Olympus) with a spring constant of 2 N/m and a resonance frequency of 70 kHz were used for all imaging.

Protein complex volumes were calculated by summing the height at each pixel inside a circle around the mass center of a protein complex as described [4]. The percentage of UvrA dimers was calculated as described [24]. The percentage of site-specific binding and the specificity of UvrA for DNA ends and DNA damage were calculated as described [25].

RESULTS

In the presence of ATP the ID contributes to damage specific binding

To understand the function of the ID in *E. coli* UvrA, we studied the activity of a mutant (UvrA ΔID) in which the entire domain is replaced by a flexible GT-linker. This mutant is similar to the UvrA ΔID mutants described in previous studies [12,14]. We started our analysis by determining the contribution of the ID to the stability of the UvrA dimer, using AFM. Both in the presence and in the absence of ATP UvrA ΔID formed a similar percentage of dimers as UvrA wildtype (Table 1), indicating that the ID does not play a role in dimerization.

Table 1: Dimer formation of UvrA wildtype and mutants

UvrA	cofactor	
	None	ATP
wildtype	29 ± 4 %	67 ± 2 %
ΔID	36 ± 4 %	73 ± 4 %
RR	29 ± 1 %	69 ± 2 %
ZnG	20 ± 4 %	23 ± 1 %
F755A	21 ± 3 %	46 ± 4 %

The (mutant) UvrA protein (20 nM) was incubated in AFM-endo buffer (with or without 1 mM ATP) for 5 minutes at 37 ºC prior to deposition on mica for AFM visualization. The percentage of UvrA dimers was calculated as described [24]. The presented values represent the average (± S.D.) of at least two independent experiments. The results for UvrA wildtype were taken from [4].

Next, we investigated the role of the ID in DNA binding and damage recognition. The damage specificity of (mutant) UvrA was determined with AFM, using a 678 bp DNA substrate, with or without a specific damage (Figure 2). The DNA affinity of (mutant) UvrA was analyzed with gel retardation assays, using the same 678 bp substrate as used in the AFM experiments (radioactively labeled at the 5'-side). As shown before [4,10], when using the undamaged fragment, on the AFM images a significant fraction of the UvrA-complexes bound the ends of the DNA (Figure 3A). Likely, UvrA recognizes DNA ends because they are slightly unwound. In the presence of ATP, the percentage of UvrA ΔID-complexes detected at the DNA ends (41 %) was lower than for the wildtype protein (52 %) (Figure 3A).

This indicates that, similar to what was observed for the *D. radiodurans* UvrA2 protein lacking the ID [14], the absence of this domain results in an enhanced binding to undamaged DNA.

This was confirmed by analyzing the affinity of UvrA ΔID for undamaged DNA by gel retardation. For the wildtype protein few complexes were detected on undamaged DNA (Figure 4A, lanes 1-2). Apparently the UvrA-complexes at the end of a DNA fragment are too instable to be detected in this assay. With UvrA ΔID however, not only more complexes were visible, but also higher-order complexes appeared, indicative for the binding of multiple UvrA dimers to the same DNA fragment (Figure 4A, lanes 3-4). This shows that the mutant indeed has a higher affinity for undamaged DNA than the wildtype protein.

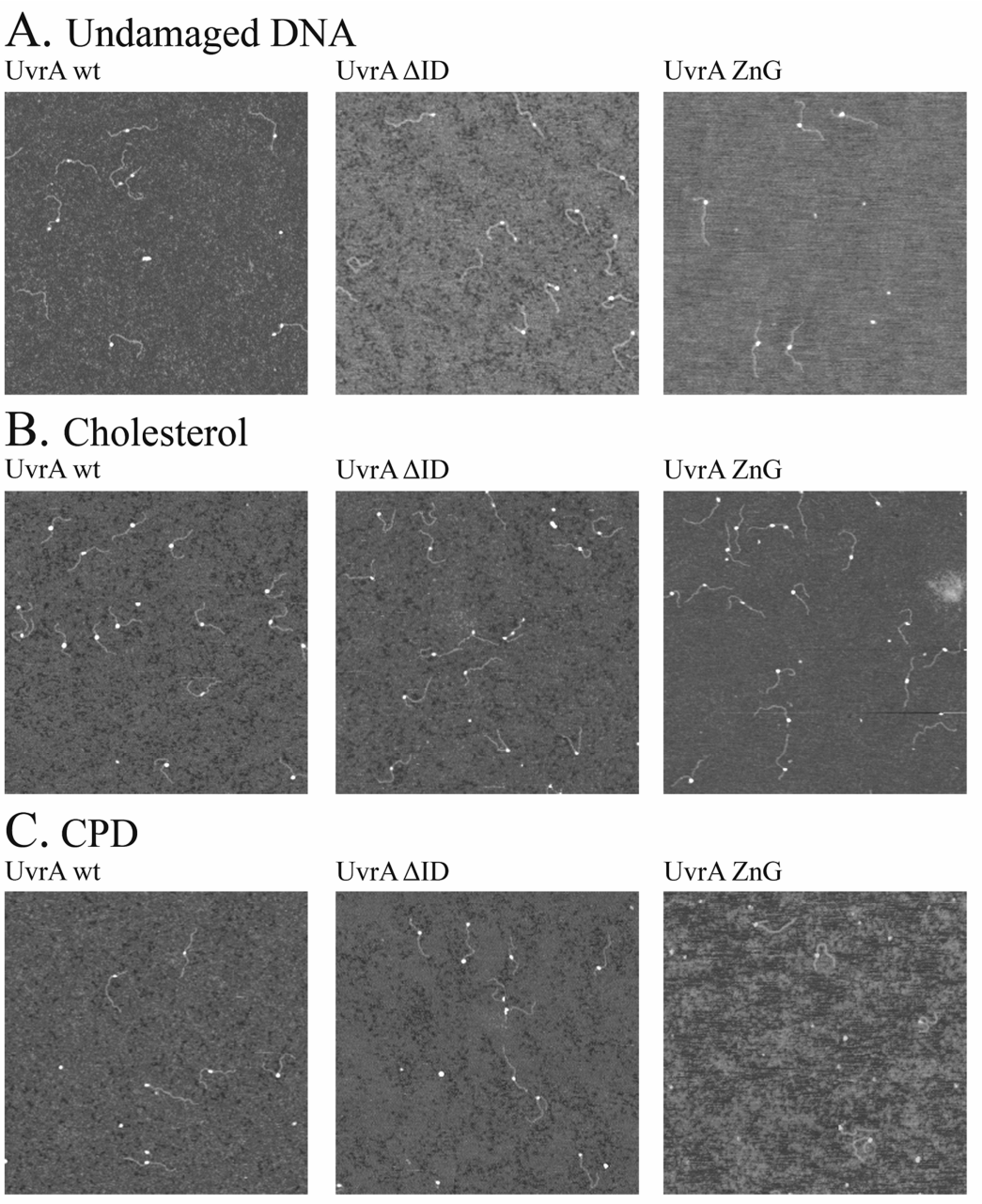

Figure 2: Representative AFM images (size 1 × 1 μm) of (mutant) UvrA-complexes on 678-bp undamaged DNA (**A**) and on the same 678-bp DNA fragment with a Cholesterol (**B**) or a CPD lesion (**C**) in the center of the substrate. All images show (mutant) UvrA incubated with ATP.

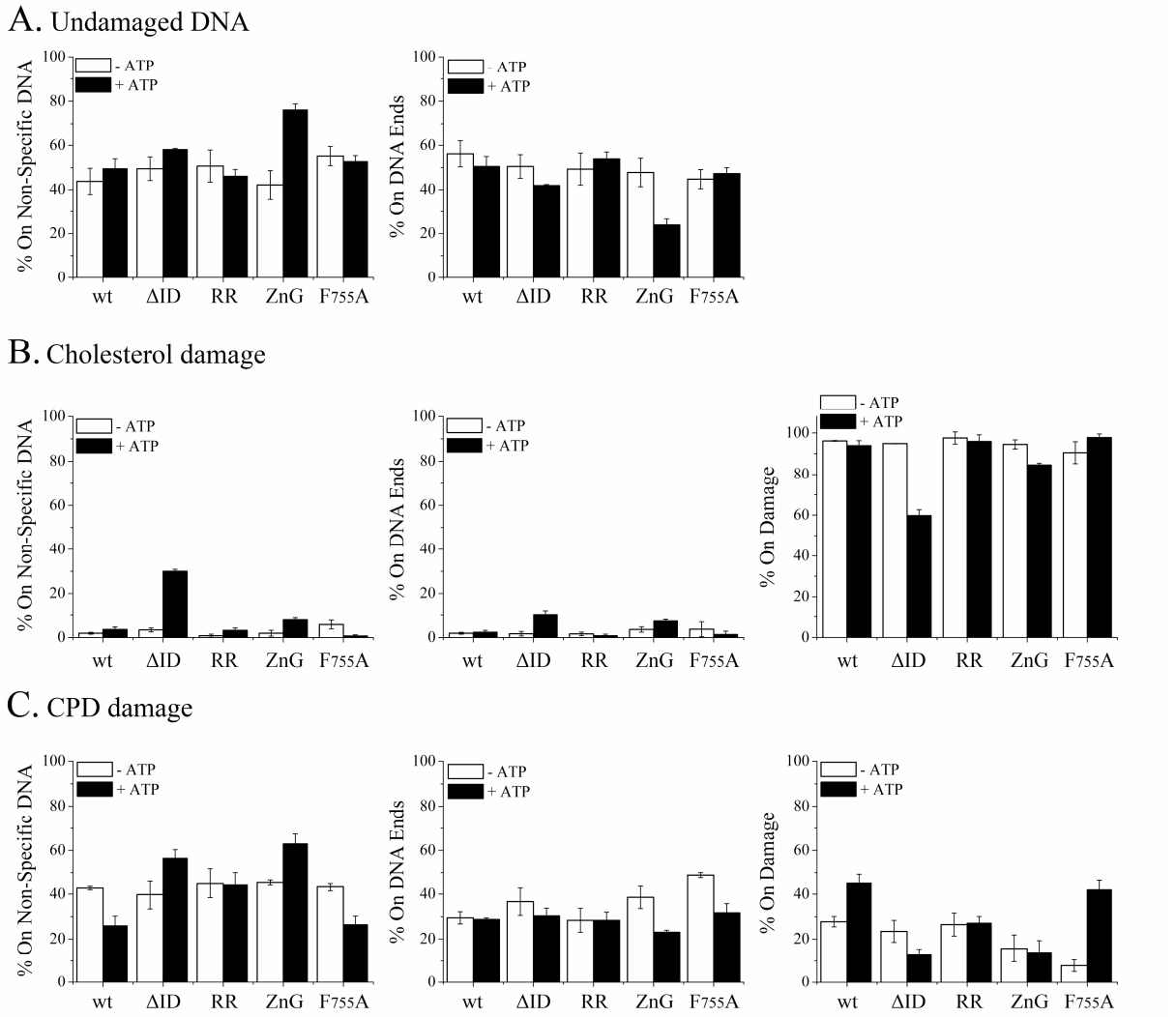

Figure 3: Quantitative analysis of UvrA-DNA complexes visualized by AFM

20 nM UvrA was incubated with 50 ng of a 678 bp DNA fragment in AFM-endo buffer. For experiments in the absence of a cofactor, 50 nM UvrA was used for the mutants UvrA ΔID, UvrA ZnG and UvrA F755A. After incubation, the complexes were deposited on freshly cleaved mica and imaged with AFM. The percentage of UvrA bound at the lesion site, DNA ends and undamaged DNA was calculated as described [25]. The presented values represent the average (± S.D.) of at least two independent experiments. Panel (**A**) shows the distribution of UvrA-complexes on undamaged DNA; (**B**) the distribution of UvrA on Cholesterol-DNA and (**C**) the distribution on CPD-DNA. The distribution of UvrA-complexes was determined in the presence (black bars) and absence (white bars) of ATP.

The increased binding of UvrA ΔID to undamaged DNA predicted that this mutant should have a lower specificity for internal lesions as well. Indeed, when using a 678 bp substrate containing a single Cholesterol lesion at the center of the DNA, in the presence of ATP a significantly lower amount of the UvrA ΔID-complexes (60 %) bound to the lesion than with wildtype UvrA (94 %) (Figure 3B).

In the gel retardation assay however, using the same conditions, UvrA ΔID bound the 678 bp Cholesterol substrate with similar affinity as wildtype UvrA (Figure 4B, lanes 1-4). This is again similar to the results obtained by Timmins *et al.* [14] for the UvrA2 ΔID mutant. The authors concluded from this experiment that in the absence of the ID UvrA can no longer discriminate between a damaged and a non-damaged site. The gel, however, does not reveal whether UvrA has bound an undamaged site or a lesion. Therefore, this assay can only be used to determine the overall affinity of (mutant) UvrA for DNA. For determination of the damage specificity AFM analysis is much more suitable, which revealed that the ΔID mutant does show preference for binding a lesion albeit with lower efficiency than wild type. The AFM technique on the other hand, is less useful for measuring DNA affinity, since protein-DNA complexes are more readily deposited on the mica than free DNA.

From the percentage of complexes on damaged and undamaged DNA detected with AFM (Figure 3), the relative specificities of (mutant) UvrA for Cholesterol-DNA and DNA ends were calculated (as described in [25]). In the presence of ATP the relative specificity of wildtype UvrA was 400 for DNA ends and 15,000 for the Cholesterol lesion. UvrA ΔID however had a relative specificity of 240 for DNA ends and 1,350 for Cholesterol-DNA, which indicates that UvrA ΔID is 10 times less specific for Cholesterol than UvrA wildtype, but only 2 times less specific for a DNA end. This suggests that the reduced damage specificity of UvrA ΔID in the presence of ATP is not only due to the mutant having a higher affinity for undamaged DNA, but also because it is affected in binding the lesion itself. We have previously shown that the binding mode at a DNA end is different from binding an internal lesion. On DNA ends only one subunit of the UvrA dimer contacts DNA, whereas on internal lesions both subunits of the UvrA-dimer bind DNA [4]. The more reduced specificity of UvrA ΔID for internal lesions therefore could indicate that the ID contributes more to DNA binding when both subunits of the UvrA dimer are involved.

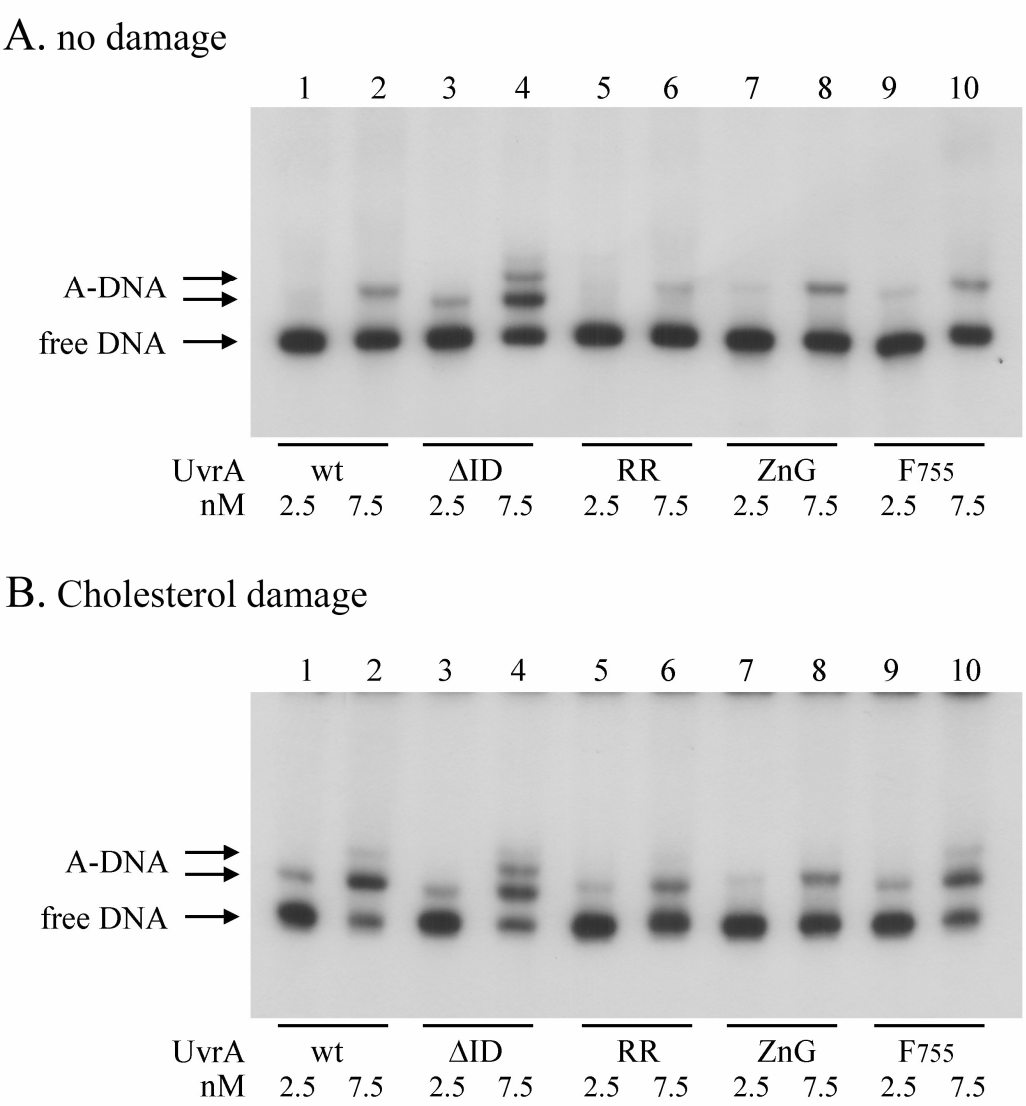

Figure 4: DNA binding activity of UvrA in the presence of ATP

The indicated amounts of UvrA were incubated with 0.4 nM DNA without damage (**A**) or containing a Cholesterol lesion (**B**) in UV-endo buffer containing 1 mM ATP. The reaction mixtures were separated on a 3.5 % polyacrylamide native gel containing 10 mM $MgCl_2$ and 1 mM ATP. Arrows indicate the position of UvrA-bound and free DNA. Because of its smaller size, the UvrA ΔID-DNA complex has a slightly faster mobility than the complex of UvrA wildtype.

In the absence of ATP the ID stabilizes UvrA on DNA

The affinity and damage specificity of UvrA ΔID was also determined in the absence of a cofactor. In this condition, UvrA wildtype had a slightly lower affinity for undamaged DNA and Cholesterol-DNA, than in the presence of ATP (Figures 4 and 5, lanes 1-2). Likely, this lower affinity is a consequence of its reduced dimerization in the absence of a cofactor (Table 1), which lowers the amount of UvrA-complexes that are available to bind DNA.

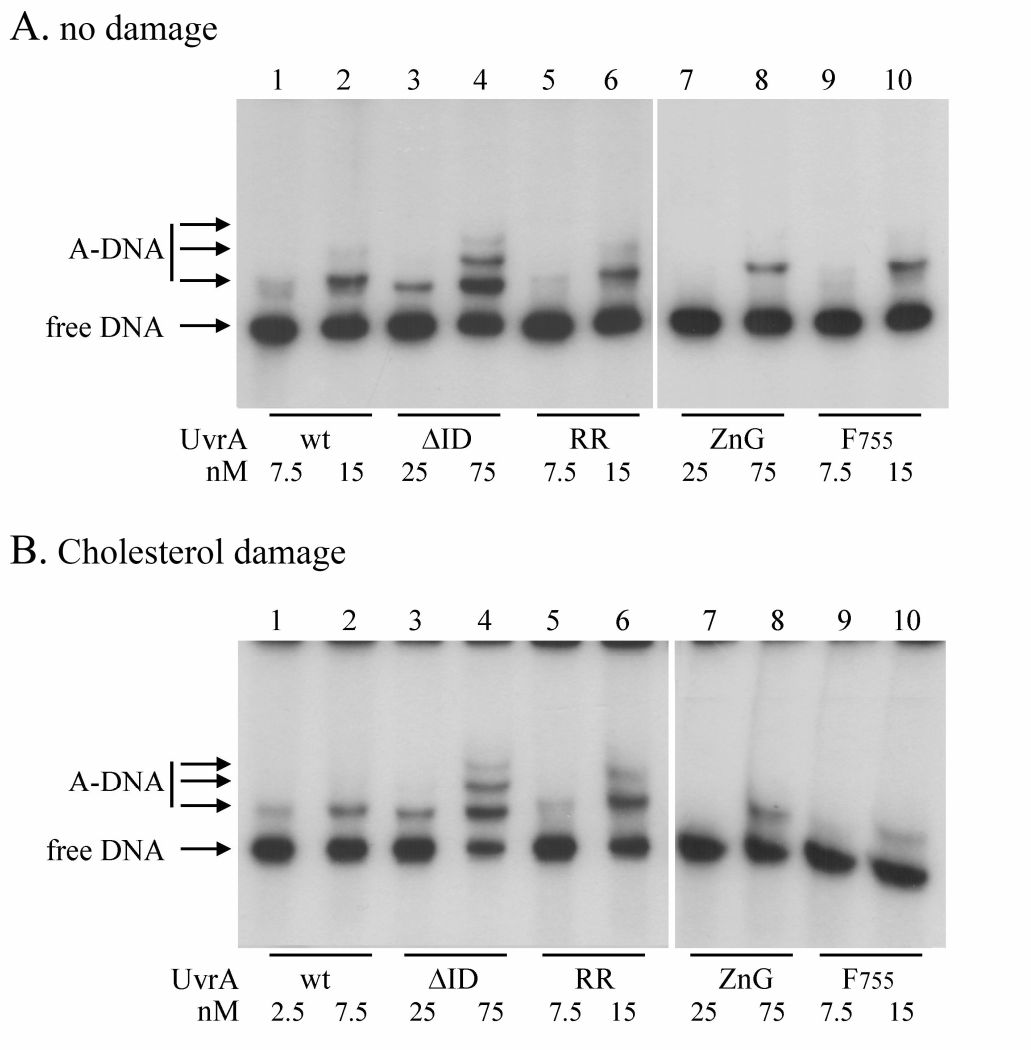

Figure 5: DNA binding activity of UvrA in the absence of a cofactor

The indicated amounts of UvrA were incubated with 0.4 nM DNA without damage (**A**) or containing a Cholesterol-lesion (**B**) in UV-endo buffer. The reaction mixtures were separated on a 3.5 % polyacrylamide native gel (containing 10 mM $MgCl_2$). Arrows indicate the position of UvrA-bound and free DNA. Because of its smaller size, the UvrA ΔID-DNA complex has a slightly faster mobility than the complex of UvrA wildtype. For the ΔID and ZnG mutants a higher concentration of protein was used.

Remarkably, the absence of a cofactor had a much stronger effect on the DNA binding of UvrA ΔID. This mutant showed a greatly reduced affinity (approximately 5-fold) for undamaged DNA and Cholesterol-DNA compared to wildtype UvrA (Figures 5A and 5B, lanes 1-4). Since in the absence of a cofactor dimerization of UvrA ΔID and of UvrA wildtype are similar (Table 1), this result indicates that the ID is important for stabilizing the UvrA-DNA complex when no cofactor is present.

Next, we tested the specificity of UvrA ΔID for DNA ends and Cholesterol with AFM using the same conditions. Due to its reduced DNA affinity, a higher concentration (50 nM) of UvrA ΔID was needed in the incubations.

As shown before [4,10], the absence of a cofactor did not affect the specificity of wildtype UvrA for DNA ends or the Cholesterol lesion (Figures 3A and 3B). In contrast to what was found when ATP was present, in the absence of cofactor UvrA ΔID had similar specificities for DNA ends and Cholesterol as wildtype UvrA (Figures 3A and 3B).

These results show that in the absence of a cofactor the ID does contribute to the stability of the UvrA-complex, but not to damage-specific binding. The difference between the role of the ID in the absence and presence of ATP indicates that the position of the ID changes as a consequence of ATP binding and/or hydrolysis.

The arginine residues in the ID contact DNA

The results shown above suggest that the ID of UvrA acts as a DNA binding domain. Remarkably, the size and amino acid content of this domain are poorly conserved between different UvrA homologs [17]. However, in the ID of *D. radiodurans* UvrA2 a few positively charged residues were identified that contributed to DNA binding [14]. Also in *E. coli* UvrA, the ID contains positively charged residues, of which residues R383 and R384 are conserved between UvrA homologs. In the structure of UvrA, these residues are positioned on the concave side of the ID (Figure 1). To determine the function of these residues, we analyzed the activity of a mutant in which residues R383 and R384 were both substituted with alanine (UvrA RR).

Similar to UvrA ΔID, UvrA RR is not affected in dimerization, either in the presence or in the absence of ATP (Table 1). In contrast to UvrA ΔID however, in the presence of ATP UvrA RR did not show enhanced binding to undamaged DNA. Instead, UvrA RR had an approximately 2-fold reduced affinity for the undamaged substrate, compared to the wildtype protein (Figure 4A, lanes 5-6). Apparently, enhanced binding to undamaged DNA occurs only when the complete ID is removed and not when individual residues are substituted.

In the presence of ATP, UvrA RR also bound Cholesterol-DNA with a lower affinity than wildtype UvrA (Figure 4B, lanes 5-6). This indicates that the arginine residues within the ID stabilize the UvrA-DNA complex on both damaged and undamaged DNA. When we looked at site-specific binding under the same conditions, UvrA RR had a similar specificity for DNA ends (Figure 3A) and Cholesterol-DNA (Figure 3B) as wildtype UvrA. Apparently, in the presence of ATP the charged residues in the ID stabilize the complex on DNA, but are not needed for recognition of the Cholesterol lesion.

In the absence of a cofactor UvrA RR had a slightly lower affinity for undamaged DNA and Cholesterol-DNA than UvrA wildtype, but the effect of removing the arginine residues on DNA affinity was not as drastic as removing the entire ID (Figures 5A and 5B, lanes 1-6). This result indicates that also in the absence of a cofactor the two arginine residues in the ID contact DNA and stabilize the UvrA-DNA complex. AFM analysis revealed that under the same conditions UvrA RR had a similar specificity for DNA ends (Figure 3A) and Cholesterol lesions (Figure 3B) as wildtype UvrA. This demonstrates that, similar to UvrA ΔID, UvrA RR is not affected in damage recognition in the absence of a cofactor.

In summary, our results show that the positively charged residues within the ID contact the DNA; thereby stabilizing the UvrA-DNA complex both on damaged and undamaged DNA. In the presence of ATP deletion of the entire ID resulted in a higher affinity of UvrA for undamaged DNA. This was also observed by Timmins *et al.* [14] for the *D. radiodurans* UvrA2 ΔID mutant. The authors ascribed this to an increased accessibility for DNA of the positively charged patches on the ventral surface of the UvrA dimer, which have been identified as DNA-binding regions [12]. Apparently, the interaction of the ID with the DNA prevents or reduces the contacts of the DNA with these positively charged regions. In the absence of ATP removal of the ID did not increase affinity for undamaged DNA, but resulted in a drastic reduction in DNA binding. This indicates that when no cofactor is bound the conformation of the UvrA dimer is such that the positively charged patches can no longer make a stable contact with the DNA; as a consequence the ID becomes much more important to prevent dissociation from the DNA.

The contact of the ID with DNA stabilizes the UvrA-complex on a non-bulky lesion

The contribution of the ID to DNA binding and damage recognition changes with the presence or absence of ATP. Previously, we have shown that ATP stabilizes the specific binding of UvrA to non-bulky lesions [10]. To investigate the contribution of the ID to binding this kind of DNA damage, the specificities of the two ID mutants for CPD-lesions were determined.

Similar as on Cholesterol-DNA, UvrA ΔID and UvrA RR are not disturbed in recognizing the CPD lesion in the absence of a cofactor; with both mutants and wildtype, approximately 27 % of the complexes were bound to the CPD lesion (Figure 3C).

In contrast to wildtype UvrA, however, both ID mutants no longer showed ATP-stimulated recognition of the CPD lesion (Figure 3C). The specificity of UvrA ΔID for CPD-DNA was even reduced in the presence of ATP.

This however was also observed for the Cholesterol lesion and could partly be ascribed to the enhanced affinity for undamaged DNA and partly to the stabilizing effect of the ID when UvrA is bound to a lesion. For this mutant the effect of binding a bulky or non-bulky lesion therefore does not appear to be significantly different. For the RR mutant, however, a damage-specific effect can be observed. On the Cholesterol lesion the RR mutant showed the same affinity as the wild type protein, but in contrast to wildtype UvrA recognition of the CPD was no longer stimulated by ATP. A similar effect has previously been found for UvrA mutant K37A, which has a mutation in ATPase domain I and which no longer hydrolyzes ATP [10].

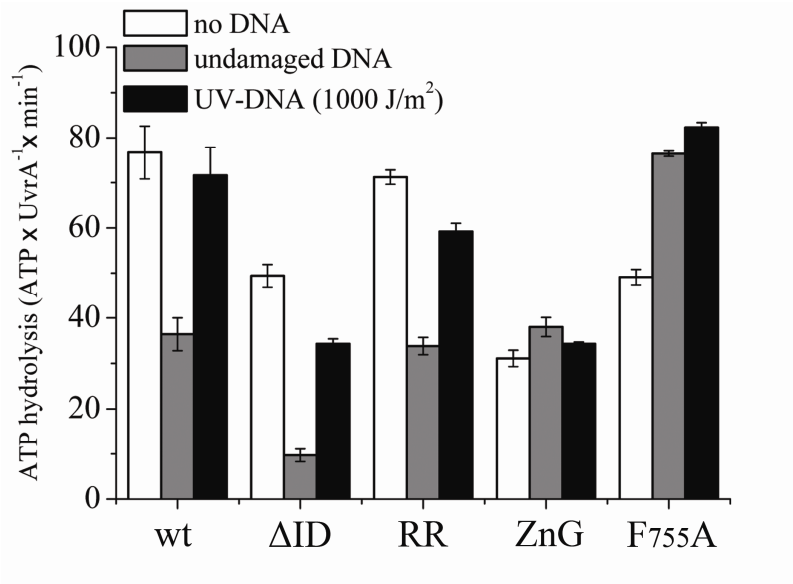

Figure 6: ATPase activities UvrA wildtype and mutants

30 nM UvrA was incubated in ATPase-endo buffer containing 0.5 mM ATP for 20 minutes at 37 ºC as described in Materials and Methods. ATPase activity of UvrA was measured by counting the total amount of ^{32}P-phosphate released from γ-^{32}P-ATP. These values were corrected for the amount of ^{32}P-phosphate released in the absence of protein. The presented values show the average ATP turnover rate (± S.D.) of (mutant) UvrA in ATP·UvrA^{-1}·min^{-1}.

To determine whether there is a correlation between the ATPase of UvrA and the contact of the RR-residues with DNA, we compared the ATPase activities of UvrA RR and wildtype UvrA in the presence and absence of (damaged) DNA. The intrinsic ATPase of wildtype UvrA is reduced upon binding to undamaged DNA and enhanced when binding to UV-damaged DNA (Figure 6). Apparently, when UvrA scans undamaged DNA for the presence of lesions ATP hydrolysis is inhibited, but when UvrA encounters a DNA lesion the ATPase is activated. The ATPase activity of UvrA RR showed a similar pattern as wildtype, hydrolysis was inhibited in the presence of undamaged DNA and stimulated by UV-irradiated DNA (Figure 6).

This clearly shows that the inability of this mutant to stabilize the UvrA-complex on the CPD lesion is not due to a defect in triggering ATP hydrolysis upon binding a UV-induced lesion. Apparently, the contact of the arginine residues with DNA becomes important after UvrA has bound a DNA lesion and its ATPase has been activated. Previously, we have suggested that the ATP-stimulated stabilization of UvrA on a CPD is the result of local unwinding of DNA around the lesion by UvrA, which is initiated by ATP hydrolysis [10]. The effect of the RR mutant on the recognition of CPD-DNA therefore strongly suggest that, after ATP hydrolysis, the interaction of the arginine residues of the wild type protein with damaged DNA results in this proposed separation of the DNA strands.

When the entire ID is deleted, the ATPase of UvrA also still responds to DNA binding as the ATPase of UvrA ΔID was reduced in the presence of undamaged DNA and stimulated when binding UV-DNA (Figure 6). Apparently, the ID is not directly involved in the coupling of ATP hydrolysis with DNA binding. Undamaged DNA had a stronger reducing effect on the ATPase of UvrA ΔID (5-fold) than on wildtype UvrA or UvrA RR (2-fold) (Figure 6). This is most likely the consequence of the observed enhanced affinity of UvrA ΔID for undamaged DNA. As with UvrA ΔID significantly less protein is found at the damaged site, it could be expected that also the damage-induced ATPase of this mutant would be lower. The ATPase of UvrA ΔID was however stimulated 3-fold in the presence of UV-irradiated DNA, which is even slightly higher than for wildtype UvrA (2.2-fold) (Figure 6). This suggests that initially UvrA ΔID does bind a lesion, where its ATPase is activated. When the ID is lacking, however, this ATPase does not result in stabilization, but instead in the dissociation of the UvrA dimer from DNA. Multiple attempts to load UvrA onto the damaged site then lead to the observed increased ATPase activity.

Presumably, after ATP hydrolysis the conformation of the UvrA dimer changes such that the interaction with the DNA binding patches on the ventral surface is reduced. As a consequence interaction with the ID becomes critical to prevent dissociation from the DNA. As shown above, the two arginine residues contribute to the interaction of the ID with DNA after ATP hydrolysis. The UvrA RR mutant however does not dissociate from the Cholesterol lesion after ATP hydrolysis, indicating that additional residues of the ID help to stabilize the UvrA complex on the DNA. Alternatively the role of the ID might be more passive by forming a clamp around the DNA helix, thereby preventing dissociation without making extensive contacts with the DNA strands.

Remarkably, UvrA ΔID also had reduced ATPase activity in the absence of DNA (Figure 6). Since this mutant was not affected in dimerization (Table 1) the residual ATPase of UvrA ΔID is apparently still sufficient to form dimers. It is not clear why the intrinsic ATPase of UvrA ΔID is reduced, but since the ATPase of UvrA is coupled to the function of the ID, it is conceivable that *vice versa* the removal of the ID influences the ATPase activity.

The zinc-finger motif of UvrA stabilizes the dimer interface

Our analysis showed that the role of the ID is dependent on binding and/or hydrolysis of ATP. Because the ID is inserted into ATPase domain I of UvrA, this ATPase domain is likely responsible for regulating the function of the ID. Also ATPase domain II of UvrA contains an insertion, the zinc-finger motif, suggesting that the function of this motif could be controlled by the ATPase of UvrA as well. To analyze the role of the zinc-finger motif, we have studied the activities of two UvrA mutants: UvrA ZnG and UvrA F755A. In UvrA ZnG, which is similar to the UvrA ZnG mutants of the *B. caldotenax* UvrA [16] and *D. radiodurans* UvrA2 homolog [14], the entire motif was deleted and replaced with a single glycine. In UvrA F755A only the conserved phenylalanine residue located at the extreme tip of the zinc-finger motif was substituted with alanine. In the structure of UvrA, the zinc-finger lies at the dimer interface, with the F755 residues of both monomers positioned closely together (Figure 1B).

We started our analysis by determining the contribution of the zinc-finger motif to formation of UvrA dimers. In the absence of ATP, with either UvrA ZnG or UvrA F755A dimerization is somewhat reduced (Table 1). More strikingly however, dimerization of UvrA ZnG was no longer stimulated by ATP (Table 1). This cannot be ascribed to the inability of UvrA ZnG to hydrolyze ATP, as in the absence of DNA UvrA ZnG did show ATPase activity, albeit with a lower rate than wildtype UvrA (Figure 6). This shows that on one hand the dimerization interface of the mutant is altered such that activation of the ATPase is less. On the other hand it shows that when ATP is hydrolyzed it does not lead to stabilization of the interface. Dimerization of UvrA F755A was enhanced by ATP, but to a lesser extent than with wildtype (Table 1) and also this mutant shows a somewhat reduced ATPase activity (Figure 6).

Apparently in this mutant the dimer interface is altered as well, but stabilization by the ATPase still (partially) occurs. Altogether, these results show that the zinc-finger motif is an important part of the dimer interface, in particular when ATP is present.

The zinc-finger coordinates the two subunits in the UvrA dimer

Dimerization of UvrA is important for its function in repair, as only dimeric UvrA-complexes stably associate with DNA [4]. Furthermore it was proposed that to bind a DNA lesion, both subunits of the UvrA dimer need to contact the DNA flanking the lesion [4]. This implies that a reduced stability of the UvrA dimer should have consequences for DNA binding and damage recognition. Therefore, we analyzed the DNA affinity and damage-specificity of the two zinc-finger motif mutants.

First, the stability of DNA binding of both mutants was analyzed in the absence of a cofactor. Under this condition, UvrA ZnG had an approximately 10-fold lower affinity for both damaged and undamaged DNA than wildtype UvrA (Figures 5A and 5B, lanes 7-8). The lower binding of UvrA ZnG cannot solely be explained by a lower amount of available dimers, since DNA binding of this mutant (10-fold reduction) was much more affected than its dimerization (1.5-fold reduction). Moreover, UvrA F755A, which in the absence of a cofactor showed a similar dimerization as UvrA ZnG, had a much higher affinity for (damaged) DNA than UvrA ZnG and overall showed only slightly less DNA binding than wildtype UvrA (Figures 5A and 5B, lanes 7-10). Apparently the absence of the zinc-finger motif in the dimer interface results in a conformation of the UvrA dimer which is less favourable for DNA binding. Notably such a reduced affinity for DNA in the absence of cofactor was also observed for the UvrA ΔID mutant (Figures 5A and 5B, lanes 3-4).

With AFM, site-specific binding of the two zinc-finger motif mutants in the absence of cofactor was investigated. Both mutants appeared significantly affected in recognizing a CPD lesion (Figure 3C), but the specificity for the Cholesterol lesion was not different from wildtype UvrA (Figure 3B). Possibly, the mutations not only reduce the stability of the UvrA dimer, but they could also affect the relative positioning of the two monomers in the dimeric complex. On a damaged site both subunits of UvrA are expected to contact the DNA flanking the lesion. Simultaneous binding of both subunits requires a proper orientation of these subunits in the dimer, explaining why the dimerization mutants show a reduced binding to the CPD lesion. The Cholesterol lesion is a much more favourable substrate for UvrA, most likely because the larger distortion of this type of lesion facilitates the contacts with the flanking DNA. This might be the reason that the effect of an altered positioning of the monomers cannot be detected on the Cholesterol lesion.

In the absence of a cofactor, the percentage of UvrA ZnG or UvrA F755A on DNA ends was also similar to that of wildtype UvrA (Figure 3A). This is not unexpected, as for binding a DNA end only one subunit of the UvrA dimer needs to contact the DNA.

Therefore, recognition of DNA ends is expected to be less dependent on the orientation of the two subunits in the UvrA dimer.

The zinc-finger motif couples DNA binding to ATPase activity

Next, we tested the properties of the zinc-finger motif mutants in the presence of ATP. We started our analysis by determining the effect of (damaged) DNA on the ATPase activity of both mutants. While the ATPase of the wildtype protein is inhibited by undamaged DNA and activated by damaged DNA, the ATPase of UvrA ZnG did not respond to DNA at all (Figure 6). The mutant protein, however, did bind DNA (see below) indicating that the zinc-finger motif is required to couple DNA binding to ATP hydrolysis.

In the presence of ATP, UvrA ZnG showed a similar amount of complexes on undamaged DNA as wildtype UvrA (Figure 4A, lanes 7-8). It should however be taken into account that under these conditions UvrA ZnG is severely disturbed in dimerization. Therefore the fewer dimers of UvrA ZnG that are available actually have a higher affinity for undamaged DNA than wildtype UvrA. This was confirmed with AFM, as in the presence of ATP less UvrA ZnG complexes were detected on the ends of undamaged DNA than with wildtype UvrA (Figure 3A). Just like the reduced affinity of UvrA ZnG for DNA in the absence of a cofactor, also this enhanced binding to undamaged DNA in the presence of ATP resembles the binding properties of the UvrA ΔID. This strongly suggests that as a consequence of the altered conformation of the dimer in the ZnG mutant the ID occupies a different position, such that it can no longer contact the DNA. As a result UvrA ZnG cannot be stabilized on the DNA in the absence of a cofactor and in the presence of ATP, the ID of UvrA ZnG can no longer reduce the DNA-affinity of the DNA binding patches on the surface.

If the ID is no longer functional in UvrA ZnG, it can be expected that also damage recognition of this mutant is similar to that of UvrA ΔID. Indeed in the presence of ATP, both mutants are affected in recognition of a Cholesterol lesion (Figure 3B). The specificity of UvrA ΔID for this lesion is however much lower than that of the ZnG mutant. This difference is likely related to the different ATPase activities of the two mutants. Upon binding damaged DNA, the ATPase of UvrA ΔID is activated, which due to the lack of the ID leads to the dissociation of the UvrA-complex from the lesion. The ATPase of UvrA ZnG however does not respond to binding damaged DNA and this mutant therefore remains bound to the damaged site. The reduced specificity of UvrA ZnG for Cholesterol is then solely caused by its enhanced affinity for undamaged DNA.

The inability of UvrA ZnG to couple ATP hydrolysis to damage recognition also explains why recognition of the CPD lesion of this mutant is no longer stimulated by ATP (Figure 3C).

Remarkably, in contrast to UvrA ZnG, the ATPase of UvrA F755A does respond to DNA, but is already stimulated by undamaged DNA (Figure 6). This suggests that, when binding undamaged DNA, the conformation of this mutant resembles that of the UvrA dimer bound to damaged DNA. In the structure of UvrA, the two F755 residues are in close proximity to each other. We propose that upon binding a lesion (i.e. when both subunits contact the DNA) the two F residues move apart, which results in the activation of ATP hydrolysis. Replacing the phenylalanine residues with alanine mimics this movement, explaining why the ATPase is already activated when bound to a non-damaged site (i.e. when only one subunit contacts the DNA). Although the ATPase of UvrA F755A is 'falsely' triggered upon binding DNA, its affinity for undamaged DNA does not differ from wildtype (Figure 4A, lanes 9-10). Apparently the ATPase can only stabilize UvrA on the DNA when a DNA lesion is present. Consequently, the specificity of F755A for binding the ends of the 678-bp undamaged DNA was also unaffected (Figure 3A).

In the presence of UV-irradiated DNA, the ATPase of UvrA F755A was further increased, already indicating that this mutant is not disturbed in damage recognition. Indeed, its specificity for Cholesterol- or CPD-DNA did not differ significantly from wildtype UvrA (Figures 3B and 3C). Moreover, the damage-induced ATPase also shows that binding to an actual damage activates the ATPase more readily than binding to a non-damaged site.

The ID and the zinc-finger motif do not directly contribute to UvrB-loading

Our analysis demonstrated that the ID of UvrA stabilizes the UvrA-complex on a lesion after ATP hydrolysis. To test whether this domain is also actively involved in the subsequent step of the repair reaction, the loading of UvrB, we analysed the formation of UvrB-DNA complexes in a gel retardation assay using the same 678-bp Cholesterol DNA substrate (Figure 7).

Starting with the UvrA RR mutant, we detected a slightly reduced UvrB-loading activity (Figure 7A, lanes 14-19). However, this is directly related to the lower affinity of this mutant for DNA. With 7.5 nM UvrA RR a similar amount of UvrA complexes was found as with 2.5 nM wildtype UvrA (Figure 7A, lanes 2 and 17) and at these concentrations there was no difference in UvrB-loading. This indicates that the contact of the arginine residues in the ID with the DNA has no direct role in the loading of UvrB.

UvrA ΔID was shown to have an increased affinity for undamaged DNA. This enhanced binding was even more pronounced in the presence of UvrB, judging from the higher-order complexes that appear upon addition of UvrB and indicate multiple UvrAB-complexes binding to the same DNA (Figure 7A, lanes 12-13). Formation of these higher-order complexes was also observed on undamaged DNA (data not shown).

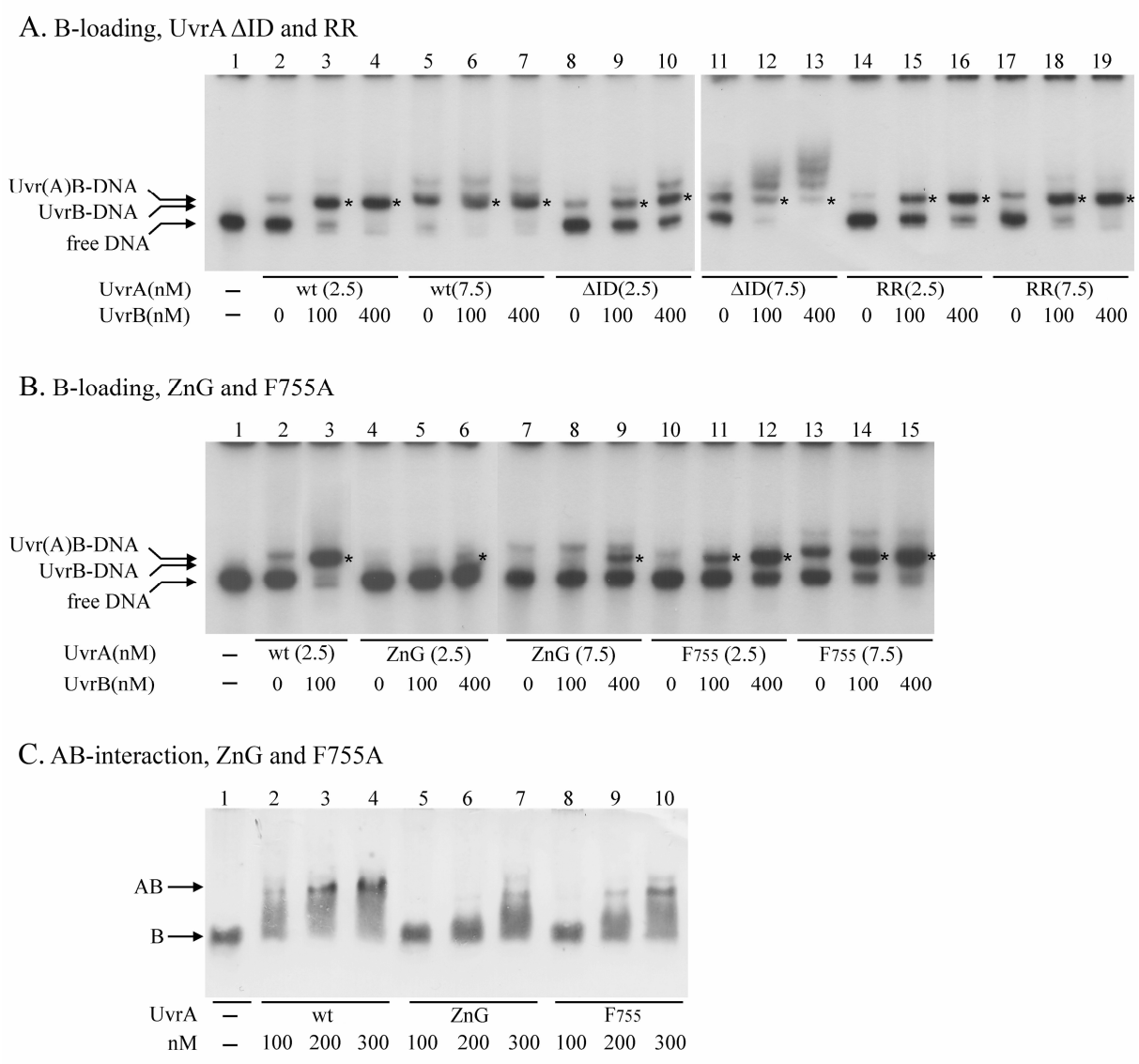

Figure 7: Analysis of the function of the ID and zinc-finger motif in UvrB-loading

(**A**, **B**) The indicated amounts of UvrA were incubated with 100- or 400 nM UvrB and 0.4 nM of the Cholesterol-containing fragment in UV-endo buffer with 1 mM ATP. The reaction mixtures were separated on a 3.5 % polyacrylamide native gel containing 10 mM $MgCl_2$ and 1 mM ATP. Arrows indicate the positions of UvrA-bound DNA, UvrB-bound DNA and free DNA. UvrB-complexes are indicated with asterisks.

(C) Western Blot showing the interaction between (mutant) UvrA and UvrB, in the presence of ATP. 100 nM UvrB was incubated with the indicated amount of UvrA in UV-endo buffer with 1 mM ATP. Reaction mixtures were separated on a 3.5 % poly-acrylamide native gel containing 10 mM $MgCl_2$ and 1 mM ATP. The gel was subsequently blotted on a nitrocellulose membrane and incubated with α-UvrB antibodies. Arrows indicate the positions of UvrB- and UvrAB-complexes.

Most likely, UvrB stabilizes the UvrA dimer and hence DNA interaction. Formation of UvrB-DNA complexes was also observed with UvrA ΔID (Figure 7A, lanes 9-10), but again this was reduced compared to the wildtype protein. This is not unexpected in view of the enhanced binding to undamaged sites, but it shows that the ID is not a prerequisite for the hand-off of the DNA to UvrB.

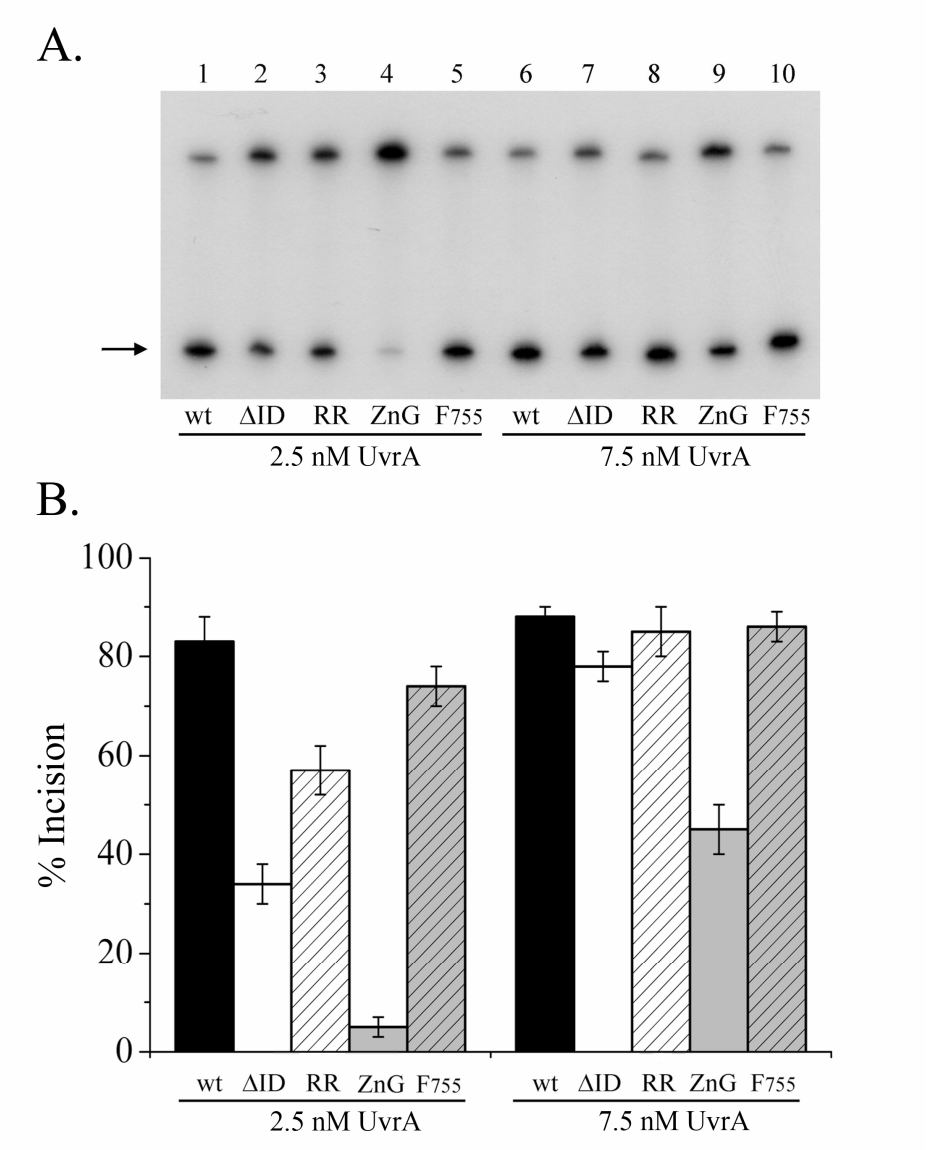

Figure 8: UvrABC incision on Cholesterol-DNA

(**A**) Visualization of DNA incision on 3.5 % denaturing polyacrylamide gels and (**B**) quantification of the percentage of incision.

2.5 or 7.5 nM (mutant) UvrA, 400 nM UvrB and 250 nM UvrC were incubated (15 min, 37 °C) with 0.4 nM Cholesterol-DNA in UV-endo buffer with 1 mM ATP. The presented values represent the average (± S.D.) of at least two independent experiments.

Also the UvrA ZnG and UvrA F755A mutants showed a reduced UvrB-loading, which can be partly rescued when using a higher concentration of UvrA (Figure 7B). This is most likely due to their reduced dimerization, as a reduced stability of the UvrA dimer will have consequences for the stability of the $UvrA_2B_2$-complex. Indeed, when testing the interaction of UvrA ZnG and UvrA F755A with UvrB in a native gel both mutants showed a reduced affinity for UvrB, which was dependent on the concentration of UvrA (Figure 7C, lanes 5-10). UvrA F755A showed a better UvrB-binding than the ZnG mutant, which correlates with F755A having a more stable dimer than UvrA ZnG.

Finally we tested the UvrABC mediated incision of the 678-bp Cholesterol-DNA in the presence of the UvrA mutants (Figure 8A). The incision assay showed the same pattern as the gel retardation assay. With UvrA ΔID and UvrA ZnG incision was reduced the most and in all cases the incision increased when a higher concentration of the mutant UvrA protein was used (Figure 8B).

Photolyase stimulates UV-survival by recruiting UvrA to CPD-lesions

We have shown that the mutations in the ID and zinc-finger motif have a more pronounced effect on UvrA binding to the non-bulky, UV-induced, CPD lesion than on binding Cholesterol-DNA. To determine the effect of the mutations on repairing UV-induced lesions *in vivo*, we analyzed the ability of *ΔuvrA E. coli* strains, carrying plasmids with the mutated UvrA gene under control of its native promoter, to survive exposure to UV-light (Figure 9). UvrA F755A, which showed a mildly affected activity *in vitro*, also showed a mildly UV-sensitive phenotype *in vivo* (Figure 9, row 11). A strain expressing UvrA ZnG was completely sensitive to UV-light (row 9), in agreement with the much reduced affinity of this protein for CPD lesions. Remarkably, although both UvrA ΔID and UvrA ZnG were similarly affected in binding a CPD lesion, the strain expressing the ΔID mutant was much more UV-tolerant than a strain expressing UvrA ZnG (Figure 9, rows 5 and 9). In addition the near wildtype level survival of bacteria containing UvrA RR is unexpectedly high in view of its reduced specificity for CPD lesions (row 7).

A clue to the cause of these discrepancies came when we repeated the UV-survival assay using a strain in which the photolyase gene is removed (*Δphr*). Photolyase is a protein that uses light to reverse CPD crosslinks. Previously, it was shown that in the absence of light photolyase cannot remove these lesions. In this condition however, photolyase is capable of stimulating the activity of UvrABC [26,27].

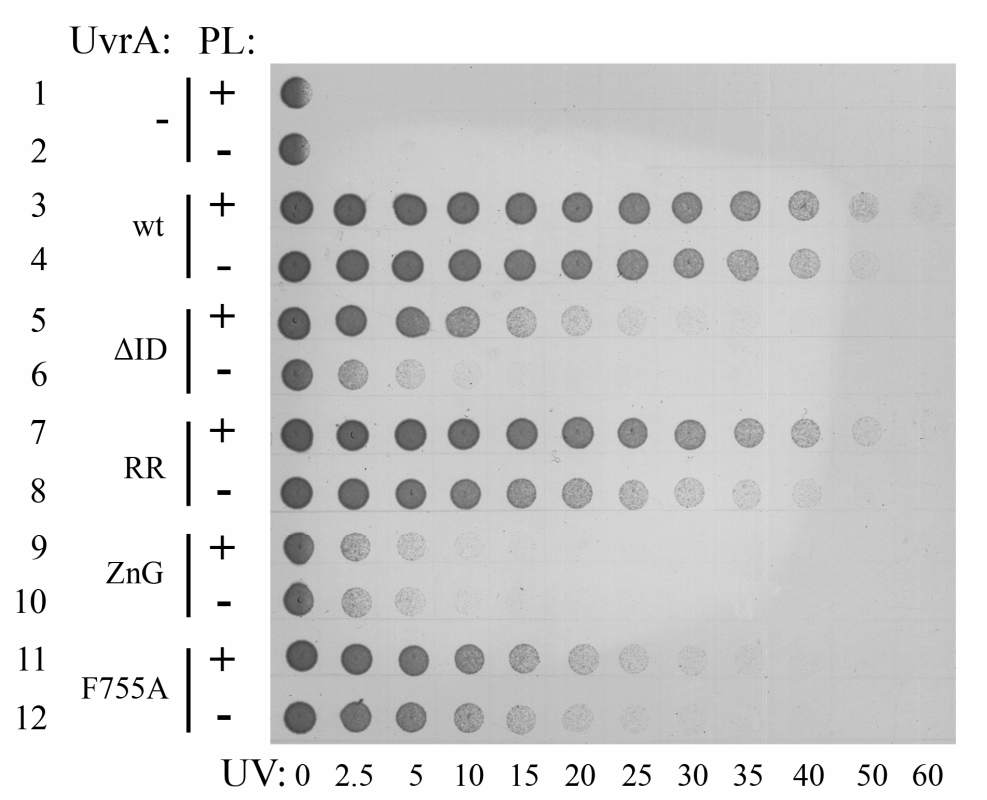

Figure 9: UV-survival of *E. coli* carrying wild-type and mutant UvrA plasmids

Δ*uvrA E. coli* strains with (+) or without the photolyase (PL) gene (-) were transformed with a plasmid carrying the (mutated) UvrA gene under control of its native promoter. Transformants (about 30,000 cells) were spotted on LB-agar plates and exposed to UV-light, after which the plates were incubated in the dark. The dose of UV-light is indicated in J/m^2.

Indeed, also in our *in vivo* assay we observed that removal of the photolyase gene slightly reduces UV-survival of a strain expressing the wildtype UvrA (Figure 9, rows 3-4). The absence of photolyase caused a similar reduction in survival of cells containing the F755A protein (rows 11-12). With the UvrA ΔID mutant however the effect of photolyase on UV-survival is much larger since the *Δphr*-strain expressing UvrA ΔID, similar to a strain expressing UvrA ZnG, was almost completely UV-sensitive (Figure 9, row 6). Apparently, the stimulating effect of photolyase on UvrABC-repair is enhanced when the ID of UvrA is missing. This strongly suggests that photolyase stimulates repair by recruiting UvrA to a CPD-site and that the ID obstructs binding of UvrA to a photolyase-bound lesion. UvrA RR was also more stimulated by photolyase, as in the *Δphr*-background survival with UvrA RR is clearly lower than with the wildtype protein (Figure 9, rows 4 and 8). This indicates that when the contact of the ID with DNA is reduced the binding of photolyase is also facilitated. For UvrA ZnG UV-survival was not stimulated at all by photolyase (rows 9-10), indicating that dimer formation is the limiting factor for this mutant, which can not be rescued by photolyase.

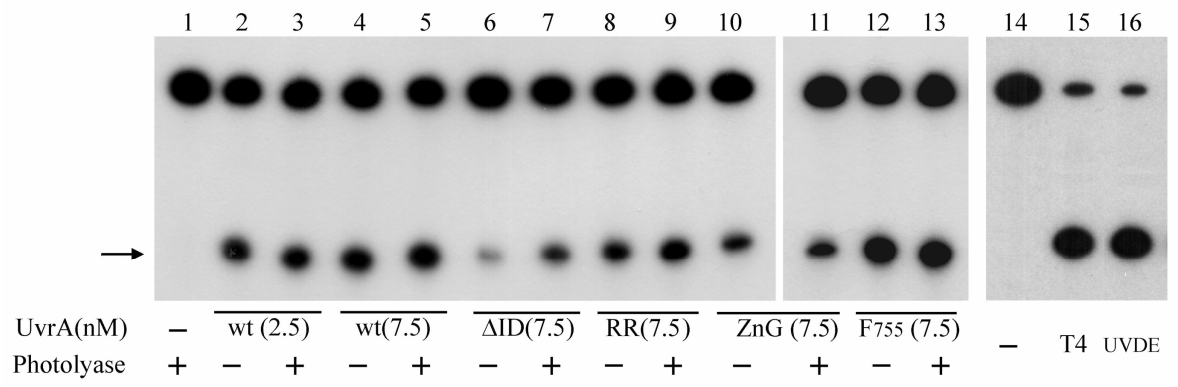

Figure 10: Stimulation of UvrABC-incision on CPD-DNA by photolyase

The indicated amount of UvrA was incubated with 400 nM UvrB, 25 nM UvrC and 0.4 nM of the CPD-DNA in UV-endo buffer with 1 mM ATP for 30 min, 37 °C. When incidated, 50 nM photolyase was added. Before the addition of UvrABC, samples containing photolyase were pre-incubated in the dark (10 min, 22 °C). The incision products were analyzed on 3.5 % denaturing polyacrylamide gels. Incision with T4-endonuclease V was done in T4-endo buffer. Incision with UVDE was performed as described [20].

We have further analyzed the interaction between photolyase and UvrABC *in vitro*, with an incision assay on the 678-bp CPD-DNA substrate. Incision activity of UvrABC on a CPD is extremely low compared to the activity of T4-endo or UVDE (Figure 10). The UvrABC-mediated incision on a CPD is also lower compared to the activity on Cholesterol-DNA (compare Figures 8 and 10). This is not unexpected as UvrA recognizes Cholesterol-DNA with a much higher specificity than CPD-DNA and also the UvrB-complex is less stable on a non-bulky lesion (data not shown). For the wild type UvrA and the ZnG and F755A mutants the stimulation of incision by photolyase was hardly detected in this assay (Figure 10). Similar as observed *in vivo*, the presence of photolyase did have a significant effect on incision in the presence of UvrA ΔID (Figure 10, lanes 6-7) or UvrA RR (lanes 8-9).

To confirm that photolyase directly stimulates binding of UvrA to the CPD lesion we determined the effect of photolyase on the ATPase activity of UvrA. To this purpose we irradiated DNA with a low UV-dose (110 J/m^2) to minimize the amount of 6-4PP lesions, which are no substrate for photolyase. Photolyase had no effect on the ATPase of UvrA in the absence of DNA or when bound to undamaged DNA (Figure 11A). On UV-irradiated DNA, however the ATPase was clearly activated by the presence of photolyase. To verify that this stimulation of ATP hydrolysis is due to binding of photolyase on CPD lesions, we pre-incubated the same substrate with photolyase in the light, allowing repair of the CPDs. Indeed, after this treatment photolyase no longer activated the ATPase of UvrA (Figure 11A). This clearly shows that photolyase stimulates NER by helping UvrA to bind UV-induced lesions.

Notably, photolyase had a more pronounced effect on the ATPase of UvrA ΔID than on the wildtype protein. When photolyase was present, the ATPase of UvrA ΔID was increased 2-fold and the ATPase of wildtype UvrA increased only 1.25-fold (Figure 11B). This confirms that removal of the ID of UvrA makes it easier for the protein to access a photolyase-bound CPD lesion.

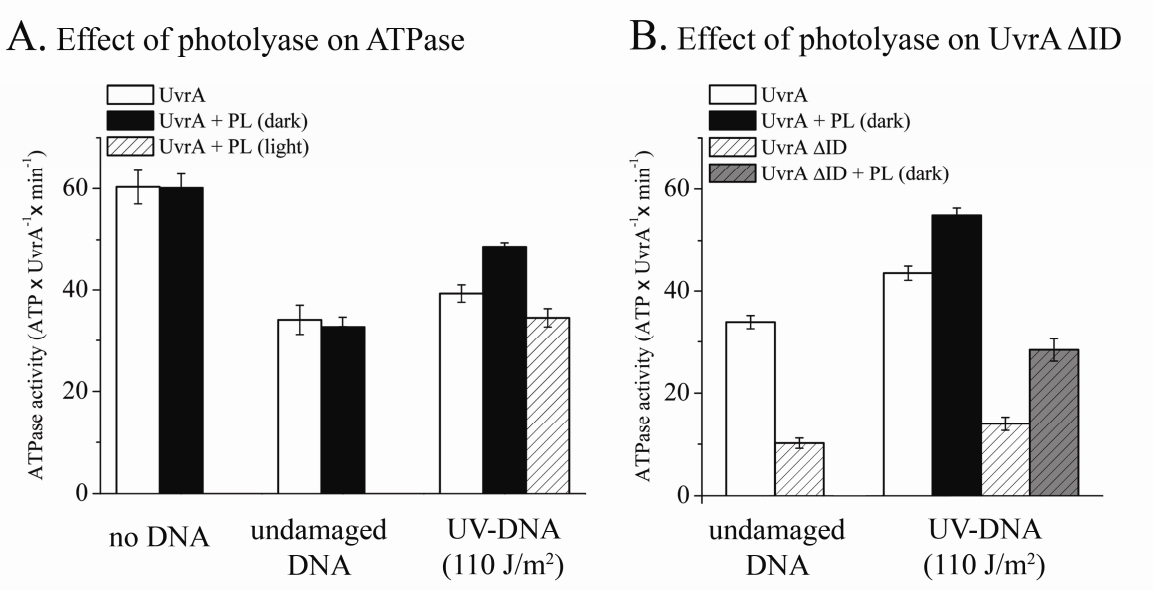

Figure 11: Stimulation of the ATPase of UvrA by photolyase

(**A**) Effect of photolyase on the activity of wildtype UvrA, in the presence or absence of (UV-irradiated) DNA.

(**B**) Effect of photolyase on the activity of UvrA ΔID

30 nM UvrA was incubated in ATPase-endo buffer containing 0.5 mM ATP for 20 minutes at 37 ºC as described in Materials and Methods. When indicated, 50 nM photolyase was added to the samples. Prior to the addition of UvrA, samples containing photolyase were pre-incubated for 10 min at 22 ºC. The presented values show the average ATP turnover rate (± S.D.) of (mutant) UvrA in ATP·UvrA^{-1}·min^{-1}.

DISCUSSION

The two ATPase domains of UvrA both belong to the family of ATP-Binding Cassette (ABC) domains, which generally consist of two functional modules: the ATPase and an insertion domain. ATP-binding and hydrolysis lead to conformational changes in the insertion domain, which for instance in ABC transporter proteins result in the transport of a compound across a membrane [28,29]. In UvrA, two ATPase domains are present. ATPase domain I contains two insertion domains, the UvrB-binding domain and the ID, whereas ATPase domain II has one insertion, the zinc-finger motif. For the UvrB-binding domain, it was already shown that its conformation is controlled by the ATPase of UvrA, as ATP binding and hydrolysis in UvrA directly affect the binding of UvrA to UvrB [10,30].

Here, we show that also the conformations of the ID and zinc-finger motif are controlled by the ATPase domains of UvrA, since the functions of these domains strongly depend on the presence or absence of ATP. The ATPase activities of the two ATPase domains of UvrA are tightly coupled, as loss-of-function mutations in one ATPase domain blocked the activity of the other domain as well [10]. This suggests that, although the ID and zinc-finger motif are inserted into different ATPase domains, the functions of these domains are also coupled.

In this paper we show that the presence of the ID is not essential for finding a damaged site, but it does stabilize the protein on the site of the lesion. This implies that other domain(s) of UvrA are involved in the actual damage discrimination. It has been shown that mutations in the positively charged patches on the ventral surface of the protein (Figure 1) reduce the affinity of UvrA for damaged DNA [12], indicating a function of these regions in damage specific binding. We propose that simultaneous binding of the DNA to both charged regions can only occur on damaged DNA (i.e., when the structure of the DNA is distorted). This can also explain how one UvrA dimer can bridge two DNA ends [4], by binding each DNA end to one of these regions. We will discuss the observations presented in this paper in light of this model, starting with the results obtained in the presence of ATP.

When bound to undamaged DNA the ID of UvrA contacts the phosphate backbone of the DNA. This became clear from the reduced stability of the UvrA-DNA complex of the RR mutant, in which two arginine residues of the ID were mutated. This implies that on the DNA the UvrA has the 'closed' conformation as shown in the crystal structure of *D. radiodurans* UvrA2 (Figure 1D). In absence of the complete ID however, the protein showed a much higher affinity for undamaged DNA. A similar increased binding to undamaged DNA was observed for a mutant of *D. radiodurans* UvrA2 lacking the ID [14]. Since the UvrA ΔID mutant could still discriminate between damaged and undamaged DNA, it is not likely that the absence of the ID now allows the undamaged DNA to contact both surface regions. Possibly, the interaction of the ID with the DNA puts a constraint on the path that the DNA has to follow along the surface of the protein. This way, the DNA is guided to both binding patches, but stable binding to these patches can only occur when DNA damage is present. When the ID is removed, this constraint is no longer present and the DNA can be in closer contact with one of the binding patches, because the adjacent DNA is no longer forced to try to contact the second region. When a lesion is present, also in the absence of ID the DNA will be able to contact the second region, making the UvrA ΔID-complex more stable on a damaged than on an undamaged site, resulting in damage specific binding.

Upon binding a lesion the ATPase of UvrA is activated. Here, we show that as a result of the ATP hydrolysis the contacts with the damaged site change. On the Cholesterol lesion this results in partial dissociation of UvrA ΔID from the site of the damage. Apparently, ATP hydrolysis alters the conformation of the DNA binding patches on the surface, possibly by changing the orientation of both monomers in the dimer. As a result, the contact of the surface region is reduced and stability of UvrA on the damaged site becomes more dependent on the contact with the ID.

This reduction of the contacts with the surface region might be important for the subsequent step of the repair reaction, the hand-off of the DNA from UvrA to UvrB. To stabilize UvrA on the damaged site, the same arginine residues of the ID are involved, as UvrA RR also had a reduced affinity for the damaged substrate. Although the ID contacts the DNA both before and after the ATPase is activated, the conformation of this domain changes upon ATP hydrolysis. This became clear from the binding of the UvrA RR mutant on the CPD lesion. We have previously shown that ATP hydrolysis of UvrA increases the specificity for CPD-DNA, whereas for a more bulky lesion ATP hydrolysis is not required [10]. Most likely the conformational change induced by the ATPase facilitates unwinding of the DNA around the lesion. The ATPase of the UvrA RR mutant however no longer stabilizes the protein on the CPD lesion, indicating that the arginine residues are directly involved in the proposed strand separation. This observation is consistent with a model where, upon ATP hydrolysis, the ID domains are repositioned into a more 'open' structure and that via the interaction of the arginine residues with the DNA backbone the two DNA strands are pulled apart. On a Cholesterol lesion the ID is required to prevent dissociation of UvrA from the lesion, but the actual ATPase-induced rearrangement of the IDs to separate the DNA strands is not needed as this intercalating lesion already causes local unwinding by itself [31].

Notably, previously presented results suggested that in UvrA from *B. stearothermophillus* the ID would have a less prominent role [12]. In this study it was shown that removal of the ID did not significantly affect UvrABC-mediated incision. It should be noted, however, that for the incision assay a relatively small (50 bp) fragment carrying a bulky (N3-Menthol) lesion was used. On such a fragment an increased affinity of the mutant for undamaged DNA will be less evident. Moreover, UvrA binding studies revealed that the *B. stearothermophillus* ΔID mutant also forms less stable complexes on a damaged site [12]. The size of the ID of *B. stearothermophillus* UvrA is very similar to that of the *E. coli* UvrA and it also contains the two conserved arginine residues.

Not all bacterial UvrA proteins, however, contain these arginine residues and also the remainder of the domain in the different UvrA homologs is very poorly conserved both in size and amino acid composition [17]. This indicates that the major role of the ID in stabilizing UvrA on the DNA is more passive, by forming a clamp around the DNA without actually making extensive contacts with the phosphate backbone.

In the absence of ATP the ID plays a much more important role in stabilizing the UvrA dimer on either damaged or undamaged DNA. Apparently, when there is no cofactor bound in UvrA the contact between the DNA binding patches on the surface of the protein and the DNA is reduced. Still, the relative orientation of these DNA binding regions do not seem altered since damage-specific binding can still occur. The significance of these results for understanding the role of UvrA in DNA repair is not exactly clear. It is very unlikely that during any of the different steps of damage searching, damage binding and loading of UvrB, the UvrA protein will be in a form where no cofactor is bound at all. The conformation of UvrA without cofactor could however mimic a conformation of UvrA during one of the stages of repair. As shown above, ATP hydrolysis by UvrA bound to a damaged site also results in reduction of the contacts of the DNA with the positively charged patches on its surface. The conformation of UvrA after ATP hydrolysis on the site of the lesion might resemble the conformation of UvrA that has no cofactor at all.

In this paper we show that the zinc-finger motif is important for dimerization of UvrA. ATP hydrolysis stabilizes the dimer of the wildtype protein [4], but when the zinc-finger motif is removed (ZnG) dimerization no longer responds to the ATPase. The zinc-finger motif is inserted in ATPase domain II of UvrA. Likely, the ATPase of this domain controls the positioning of the zinc-finger. In the crystal structure of UvrA [12] the zinc-finger motif itself does not make an extensive contact across the dimer interface. Only the phenylalanine residues at the tip of the two motifs are in close proximity (Figure 1B). Important parts of the dimeric interface are two alpha helices that are connected to ATPase domain I of UvrA. These alpha helices are located just beneath the zinc-finger motif (Figure 1B). Likely, positioning of these alpha-helices is controlled by the zinc-finger motifs and hence by the ATPase in domain II.

Deletion of the zinc-finger motif also impaired the function of the ID. This became clear from the observations that the UvrA ZnG mutant has a much reduced affinity for both damaged and undamaged DNA in the absence of cofactor and bound undamaged DNA more tightly than the wildtype protein in the presence of ATP. An increased affinity for undamaged DNA was also found for the equivalent ZnG mutant of the *B. caldotenax* UvrA [16].

The DNA binding properties of the ZnG mutant closely resemble those of UvrA ΔID, suggesting that in UvrA ZnG the ID cannot be properly positioned to contact the DNA. Since the ID and the zinc-finger motif are not structurally connected (Figure 1A) this is most likely an indirect consequence of a different positioning of the two monomers in the UvrA ZnG dimer.

The zinc-finger motif appeared to be an important mediator between DNA binding and the ATPase of UvrA. The ATPase of the wild type UvrA is inhibited when searching for the presence of damage in the DNA and is activated when a lesion is found. The ATPase of the ZnG mutant however did not respond at all to either damaged or undamaged DNA. The zinc-finger motifs are connected to the DNA binding patches on the surface of UvrA (Figure 1A). Most likely the signal of DNA binding to these regions is transmitted via the zinc-finger motifs to the alpha helices located underneath, which subsequently transmit the signal to ATPase domain I. Residue F755 at the tip of the zinc-finger motif plays a pivotal role in the transmission of this signal. When this residue is substituted with alanine, the UvrA already activates its ATPase when bound to an undamaged site. In the structure of the UvrA dimer, the two F residues (F751 in *B. stearothermophilus* UvrA) are in close proximity (Figure 1B), indicating that these residues can make a hydrophobic contact. Replacing phenylalanine with alanine disables this contact, which apparently triggers the ATPase. This suggests that binding to a damaged site also removes the contact between the tips of the zinc-finger motifs. We therefore propose the following model for damage recognition by UvrA:

When searching for damage, UvrA binds to the DNA via one of the DNA binding patches on the surface. Subsequently, the IDs will clamp around the DNA, thereby directing the DNA towards the other surface region. In this conformation the two zinc-finger motifs are connected via the F residues, which positions the alpha helices underneath such that the ATP in site I cannot be hydrolyzed. Upon the encounter of a DNA lesion, the DNA will also contact the second positively charged patch on the surface. As a result of the dual interaction, the two DNA binding regions are rearranged. Concomitantly, the zinc-finger motifs which are connected to the DNA binding regions will move, leading to disruption of the contact between the F residues. Because now the zinc-finger motifs are no longer connected, the alpha helices located underneath are rearranged and the ATPase of site I is activated. The conformational change as result of the ATP hydrolysis in site I might in its turn reposition the two monomers such that the contact of the surface regions with the DNA is reduced. In addition this triggers the movement of the ID that leads to strand separation via interaction with the conserved arginine residues.

The data described in this paper also shed more light on the mechanism behind an observation made some time ago that photolyase stimulates the activity of UvrABC on UV-induced lesions [26,27]. Here, we showed that photolyase promotes binding of the UvrA protein to a CPD lesion. Photolyase likely facilitates this by creating a larger distortion around the lesion since this protein was shown to flip the crosslinked nucleotides out of the DNA helix [32,33]. Nucleotide flipping can only occur when photolyase has bound the lesion itself, indicating that both proteins are simultaneously bound to the CPD site. Since photolyase flips the CPD into its active site [32], the lesion itself is not accessible for UvrA. This implies that UvrA binds the DNA helix on the opposite side of the CPD lesion.

Likely, UvrA binding to protein-bound lesions is not an uncommon mechanism to enhance recognition of DNA damage *in vivo*. Recently, it was shown that the alkyltransferase-like (ATL) proteins *Thermus thermophilus* TTHA1564 and *E. coli* YbaZ can bind UvrA and stimulate NER-mediated repair of alkylated DNA [34,35].

ATL-proteins are highly similar to the alkyltransferases, but lack alkyltransferase activity and therefore cannot repair alkylated DNA by themselves [36]. Instead, ATLs initiate repair through recruitment of other repair proteins like UvrA to alkylated DNA. Like photolyase, ATL proteins perform nucleotide-flipping on their substrate [37]. This suggests that UvrA binds an ATL-bound lesion in a similar way as it binds photolyase-bound CPD.

Remarkably, both *in vivo* and *in vitro*, the presence of photolyase had a stronger effect on the activities of UvrA ΔID and UvrA RR than on wildtype UvrA. Apparently when the ID is clamped around the DNA helix, it obstructs the simultaneous binding of photolyase. Interestingly, some bacterial species carry a UvrA homolog (UvrA class III) that does not contain an ID. Class III UvrA homologs are only found in bacteria that also contain a generic UvrA [17], suggesting that they do not play a primary role in NER. Possibly, the class III UvrA homologs function to initiate repair on damaged sites that are bound by ‘repair helping’ proteins such as ATL proteins or photolyases. Class III UvrAs could also contribute to repair of extremely large DNA adducts, such as peptide-DNA crosslinks. These lesions are generally poorly incised by UvrABC [38,39], but in the absence of the ID binding of UvrA to such rare lesions might be enhanced.

ACKNOWLEDGEMENTS

This work was supported by the Netherlands Organization for Scientific Research (NWO) [grant number 700.52.706]. The authors would like to thank Femke de Korte for the cloning and purification of UvrA ΔID, Auke Haanstra for cloning and purifying UvrA ZnG and F755A. Andries Eker is kindly acknowledged for his generous gift of purified *E. coli* CPD-photolyase. Tineke de Ruijter is credited for her gift of purified T4-endonuclease. Federica Galli and Tjerk Oosterkamp are kindly acknowledged for allowing our participation in the Bio-AFM lab at Leiden University.

REFERENCES

1. Van Houten, B., Croteau, D.L., DellaVecchia, M.J., Wang, H. and Kisker, C. (2005) 'Close fitting sleeves': DNA damage recognition by the UvrABC nuclease system. *Mutat. Res.*, **577**, 92-117

2. Truglio, J.J., Croteau, D.L., Van Houten, B. and Kisker, C. (2006) Prokaryotic nucleotide excision repair: The UvrABC system. *Chem Rev.*, **106**, 233-252

3. Mazur, S. and Grossman, L. (1991) Dimerization of *Escherichia coli* UvrA and its binding to undamaged and ultraviolet damaged DNA. *Biochemistry*, **30**, 4432-4443

4. Wagner, K., Moolenaar, G., van Noort, J. and Goosen, N. (2009) Single-molecule analysis reveals two separate DNA binding domains in the *Escherichia coli* UvrA dimer. *Nucleic Acids Res.*, **37**, 1962-1972

5. Verhoeven, E.E.A., Wyman, C., Moolenaar, G.F. and Goosen, N. (2002) The presence of two UvrB subunits in the UvrAB complex ensures damage recognition in both DNA strands. *EMBO J.*, **21**, 4196-4205

6. Van Houten, B., Gamper, H., Sancar, A. and Hearst, J.E. (1987) DNaseI footprint of ABC excinuclease. *J. Biol. Chem.*, **262**, 13180-13187

7. Gorbalenya, A.E. and Koonin, E.V. (1990) Superfamily of UvrA-related NTP-binding proteins. Implications for rational classification of recombination/repair systems. *J. Mol. Biol.*, **213**, 583-591

8. Myles, G.M., Hearst, J.E. and Sancar, A. (1991) Site-specific mutagenesis of conserved residues within Walker A and B sequences of *Escherichia coli* UvrA protein. *Biochemistry*, **30**, 3824-3834

9. Thiagalingam, S. and Grossman, L. (1991) Both ATPase sites of *Escherichia coli* UvrA have functional roles in nucleotide excision repair. *J. Biol. Chem.*, **266**, 11395-11401

10. Wagner, K., Moolenaar, G.F. and Goosen, N. (2010) Role of the two ATPase domains of UvrA in binding non-bulky lesions and interaction with UvrB. *DNA Repair*, **9**, 1176-1186

11. Van Houten, B., Gamper, H., Hearst, J.E. and Sancar, A. (1988) Analysis of sequential steps of nucleotide excision repair in *Escherichia coli* using synthetic substrates containing single psoralen adducts. *J. Biol. Chem.*, **263**, 16553-16560

12. Pakotiprapha, D., Inuzuka, Y., Bowman, B.R., Moolenaar, G.F., Goosen, N., Jeruzalmi, D. and Verdine, G.L. (2008) Crystal structure of *Bacillus stearothermophilus* UvrA provides insight into ATP-modulated dimerization, UvrB interaction, and DNA binding. *Mol. Cell.*, **29**, 122-133

13. Hopfner, K.P. and Tainer, J.A. (2003) Rad50/SMC proteins and ABC transporters: unifying concepts from high resolution structures. *Curr. Opin. Struct. Biol.*, **13**, 249-255

14. Timmins, J., Gordon, E., Caria, S., Leonard, G., Acajjaoui, S., Kuo, M.S., Monchois, V. and McSweeney, S. (2009) Structural and mutational analysis of *Deinococcus radiodurans* UvrA2 provide insight into DNA binding and damage recognition by UvrAs. *Structure*, **17**, 547-558

15. Croteau, D.L., DellaVecchia, M.J., Perera, L. and Van Houten, B. (2008) Cooperative damage recognition by UvrA and UvrB: identification of UvrA residues that mediate DNA binding. *DNA Repair*, **7**, 392-404

16. Croteau, D.L., DellaVecchia, M.J., Wang, H., Bienstock, R.J., Mellon, M.A. and Van Houten, B. (2006) The C-terminal zinc-finger of UvrA does not bind DNA directly but regulates damage-specific DNA binding. *J. Biol. Chem.*, **281**, 26370-26381

17. Goosen, N. and Moolenaar, G.F. (2008) Repair of UV damage in bacteria. *DNA Repair*, **7**, 353-379

18. Backendorf, C., Brandsma, J.A., Kartasova, T. and van de Putte, P. (1983) *In vivo* regulation of the *UvrA* gene: role of the "-10" and "-35" promoter regions. *Nucleic Acids Res.*, **11**, 5795-5810

19. Visse, R., de Ruijter, M., Moolenaar, G.F. and van de Putte, P. (1992) Analysis of UvrABC endonuclease reaction intermediates on cisplatin-damaged DNA using mobility shift gel electrophoresis. *J. Biol. Chem.*, **267**, 6736-6742

20. Paspaleva, K.K., Thomassen, E., Pannu, N.S., Iwai, S., Moolenaar, G.F., Goosen, N. and Abrahams, J.P. (2007) Crystal structure of the DNA repair enzyme ultaviolet damage endonuclease. *Structure*, **15**, 1163-1165

21. Moolenaar, G.F., Moorman, C. and Goosen, N. (2000) Role of the *Escherichia coli* nucleotide excision repair proteins in DNA replication. *J. Bacteriol.*, **182**, 5706-5714

22. Verhoeven, E.E.A., van Kesteren, M., Turner, J.J., van der Marel, G.A., van Boom, J.H., Moolenaar, G.F. and Goosen, N. (2002) The C-terminal region of *Escherichia coli* UvrC contributes to the flexibility of the UvrABC nucleotide excision repair system. *Nucleic Acids Res.*, **30**, 2492-2500

23. Moolenaar, G.F., Visse, R., Ortiz-Buysse, M., Goosen N. and van de Putte, P. (1994) Helicase motifs V and VI of the *Escherichia coli* UvrB protein of the UvrABC endonuclease are essential for the formation of the preincision complex. *J. Mol. Biol.*, **240**, 294-307

24. Ratcliff, G.C. and Erie, D.A. (2001) A novel single-molecule study to determine protein-protein association constants. *J. Am. Chem. Soc.*, **123**, 5632-5635

25. Yang, Y., Sass, L.E., Du, C., Hsieh, P. and Erie, D.A. (2005) Determination of protein-DNA binding constants and specificities from statistical analyses of single molecules: MutS-DNA interactions. *Nucleic Acids Res.*, **33**, 4322-4334

26. Sancar, A., Franklin, K.A. and Sancar, G.B. (1984) *Escherichia coli* DNA photolyase stimulates uvrABC excision nuclease *in vitro*. *Proc. Natl. Acad. Sci. U.S.A.*, **81**, 7397-7401

27. Sancar, G.B. (1990) DNA photolyases: Phyiscal properties, action mechanism, and roles in dark repair. *Mut. Res.*, **236**, 147-160

28. Moussatova, A., Kandt, C., O'Mara, M.L. and Tieleman, D.P. (2008) ATP-binding cassette transporters in *Escherichia coli*. *Biochim. Biophyis. Acta*, **1778**, 1757-1771

29. Seeger, M.A. and van Veen, H.W. (2009) Molecular basis of multidrug transport by ABC transporters. *Biochim. Biophyis. Acta*, **1794**, 725-737

30. Malta, E., Moolenaar, G.F. and Goosen, N. (2007) Dynamics of the UvrABC nucleotide excision repair proteins analyzed by fluorescence resonance energy transfer. *Biochemistry*, **46**, 9080-9088

31. Gómez-Pinto, I., Cubero, E., Kalko, S.G., Monaco, V., van der Marel, G., van Boom, J.H., Orozco, M. and Gonzalez, C. (2004) Effect of bulky lesions on DNA. *J. Biol. Chem.*, **279**, 24552-24560

32. Mees, A., Klar, T., Gnau, P., Hennecke, U., Eker, A.P.M., Carell, T. and Essen, L.O. (2004) Crystal structure of a photolyase bound to a CPD-like DNA lesion after in situ repair. *Science*, **306**, 1789-1793

33. Yang, K. and Stanley, R.J. (2006) Differential distortion of substrate occurs when it binds to DNA photolyase: A 2-aminopurine study. *Biochemistry*, **45**, 11239-11245

34. Morita, R., Nakagawa, N., Kuramitsu, S. and Masui, R. (2008) O^6-methylguanine-DNA methyltransferase-like protein from *Thermus thermophilus* interacts with a nucleotide excision repair protein. *J. Biochem.*, **144**, 267-277

35. Mazon, G., Philippin, G., Cadet, J., Gasparutto, D. and Fuchs, R.P. (2009) The alkyltransferase-like *ybaZ* gene product enhances nucleotide excision repair of O^6-alkylguanine adducts in *E. coli*. *DNA Repair*, **8**, 697-703

36. Margison, G.P., Butt, A., Pearson, S.J., Wharton, S., Watson, A.J., Marriott, A., Caetano, C.M., Hollins, J.J., Rukazenkova, N., Begum, G. and Santibañez-Koref, M.F. (2007) Alkyltransferase-like proteins. *DNA Repair*, **6**, 1222-1228

37. Tubbs, J.L., Latypov, V., Kanugula, S., Butt, A., Melikshvili, M., Kraehenbuehl, R., Fleck, O., Marriott, A., Watson, A.J., Verbeek, B., McGown, G., Thorncroft, M., Santibañez-Koref, M.F., Millington, C., Arvai, A.S., Kroeger, M.D., Peterson, L.A., Williams, D.M., Fried, M.G., Margison, G.P., Pegg, A.E. and Tainer, J.A. (2009) Alkylated DNA damage flipping bridges base and nucleotide excision repair. *Nature*, **459**, 808-813

38. Minko, I.G., Zou, Y. and Lloyd, R.S. (2002) Incision of DNA-protein crosslinks by UvrABC nuclease suggests a potential repair pathway involving nucleotide excision repair. *Proc. Natl. Acad. Sci. U.S.A.*, **99**, 1905-1909

39. Minko, I.G., Kurtz, A.J., Croteau, D.L., Van Houten, B., Harris, T.M. and Lloyd, R.S. (2005) Initiation of repair by DNA-polypeptide cross-links by the UvrABC nuclease. *Biochemistry*, **44**, 3000-3009